Natural Hazards
and Earth System
Sciences

Tangible and intangible ex post assessment of flood-induced damage to cultural heritage

Claudia De Lucia[1,2]**, Michele Amaddii**[1]**, and Chiara Arrighi**[1,2]

[1]Department of Civil and Environmental Engineering, Università degli Studi di Firenze,
Via di S. Marta 3, 50139 Florence, Italy
[2]Fondazione RETURN, Corso Umberto I, 40, 80138 Naples, Italy

Correspondence: Chiara Arrighi (chiara.arrighi@unifi.it)

Abstract. Floods pose significant risks to cultural heritage (CH), yet post-disaster damage data on CH remain lacking. In this paper, we address this gap by focusing on the ex post assessment of flood-induced damage to CH. The method involves the identification of damaged assets and a field survey to assess loss in tangible value (LTV) and loss in intangible value (LIV). The potential contributing factors, e.g. water depth and river slope, are analysed through geospatial analysis. Ex post damage data on CH are compared with the outcome of an ex ante analysis based on available methods to verify the quality of exposure data and possible limitations. The method is applied to the 15–16 September 2022 flood event that occurred in the Marche region (Italy). The survey involved 14 CH in 4 municipalities and 3 catchments. Results highlight the inadequacy of existing exposure data for ex ante damage assessment and the importance of building characteristics. However, ex post data confirm that religious architectures are likely to suffer the highest LTV and LIV. The ex post damage analysis provided a semi-quantitative evaluation of both LTV and LIV in relation to flood characteristics. Notably, significant correlations between LTV and flood depth, as well as with the slope of the riverbed (a proxy for river flow velocity), were found. LIV correlates well to flood depth and river slope albeit with lower R^2 and larger RMSE, highlighting that intangible impact analysis requires more effort than hazard characterization. Further research should increase the availability of ex post damage data on CH to form the basis for damage model validation and development of empirical vulnerability functions.

1 Introduction

Floods are among the most frequent and costliest natural hazards (CRED and UNISDR, 2015). In recent decades, the frequency and intensity of heavy rainfall, associated with ongoing climate change, have consequently led to an increase in flood events (Merz et al., 2021; IPCC, 2023). Moreover, due to severe urbanization and increasing development in flood-prone areas, flood impacts are expected to grow in the future (Dottori et al., 2023).

The EU Floods Directive calls upon member countries to mitigate the potential adverse consequences of flooding on human health, the environment, cultural heritage, and economic activities (EU, 2007). Concerning cultural heritage (CH), this purpose gains even more significance. Indeed, CH assets are severely affected by floods and are likely to be increasingly threatened by climate change effects (Marzeion and Levermann, 2014; Fatorić and Seekamp, 2017; Sesana et al., 2021). In many cases, substantial costs for restoration are necessary, and in the worst-case scenario, the irreversible destruction of unique and irreplaceable assets that hold cultural significance is unavoidable (Arrighi, 2021; Arrighi et al., 2023b). Furthermore, the impact of floods on CH extends beyond the tangible damage, affecting social identity and cohesion (Romão et al., 2020).

Cultural heritage can be defined as the legacy of tangible and intangible attributes inherited from past generations. Tangible attributes include buildings, monuments, and historic places, as well as works of art, literature, music, and artifacts, both archaeological and historical. Intangible attributes comprise social customs, traditions, and practices,

rooted in aesthetic and spiritual beliefs and oral traditions (Willis, 2014).

Over the past few decades, ex ante damage assessment, namely impact analysis and mitigation measures of natural hazards to CH assets, such as floods, has received considerable scientific attention. Many researchers have focused on individual assets or site levels (Sabbioni et al., 2007; Drdácký, 2010; Huijbregts et al., 2014; Figueiredo et al., 2021; Sesana et al., 2021; Momčilović Petronijević and Petronijević, 2022; Anderson, 2023). Other studies have focused on the negative effects of natural hazards on CH concerning societal impacts and economic losses (Alexandrakis et al., 2019; Garrote et al., 2020). Additionally, several studies have focused on flood risk assessment of CH at various scales, ranging from specific sites (Zhang et al., 2024) to cities (Wang, 2015; Arrighi et al., 2018, 2023a, b; Trizio et al., 2021; Schlumberger et al., 2022; Brokerhof et al., 2023; Ravan et al., 2023), regions (Godfrey et al., 2015; Figueiredo et al., 2020; Garrote et al., 2020), and national levels (Stephenson and D'Ayala, 2014), and even globally (Reimann et al., 2018; Arrighi, 2021). The ex ante analyses represent a key aspect of any flood risk management plan, as required by the EU Floods Directive (EU, 2007). However, estimating the loss after an event is equally important to support emergency management and decide priorities for reconstruction and victim compensation (Molinari et al., 2014). Furthermore, identifying key factors influencing the vulnerability of CH assets is necessary for a more robust risk assessment. Achieving this requires the availability of post-disaster loss information and data, coupled with appropriate ex post damage analyses. Such endeavours would highlight weaknesses in current risk management practices and thus improve the effectiveness of preparedness and resilience strategies (Arrighi et al., 2022). Nevertheless, there are only a few examples in the literature concerning the ex post assessment of damage to CH. In the work of Vecvagars (2006), an overview of the different available methods in assessing the value of CH assets, providing some recommendations for valuing damage and losses after a disaster, is outlined. Since 2008, the European Commission, the United Nations Development Group, and the World Bank have developed the joint Post-Disaster Needs Assessment (PDNA) tool. This tool provides a comprehensive, government-led assessment of post-disaster damage, losses, and recovery needs, paving the way for a consolidated recovery framework. The PDNA framework encompasses the gathering of data on damage to both tangible and intangible values of cultural assets. More recently, a reviewed version of the PDNA, based on experiences gathered through the analysis of many PDNA post-disaster assessments conducted since 2008, was published (Jeggle and Boggero, 2018). Vafadari et al. (2017) developed a tool for the recording and inventory of sites and monuments; the recording of damage, threats, and their causes; and for the assessment of their magnitude. Deschaux (2017) details the observed impacts on movable and immovable heritage following the floods in central France in 2016. Figueiredo et al. (2021) analyse the impacts of wildfires that occurred in Portugal on cultural heritage integrating geospatial analysis with information provided directly by municipalities affected by the wildfires.

As already mentioned, CH assets are characterized by both tangible and intangible value, and consequently, the damage they suffer can be tangible and intangible. Therefore, for an adequate assessment of flood damage to CH, a classification of these values is necessary (Romão et al., 2020), whether the analysis is conducted ex ante or ex post. Vecvagars (2006) groups cultural heritage values into "use value" (related to market value) and "non-use value" (i.e. non-market value such as spiritual value, legacy value, and social value). In addition, use value can be further divided into "extractive use value" and "non-extractive use value". Extractive use value includes consumptive value, which can be measured through market transactions. Non-extractive use value originates from the service the asset provides and includes aesthetic and recreational values.

However, it is often noted that quantitative disaster data concerning losses related to cultural heritage are either scarce or entirely unavailable (Romão et al., 2020). This underscores the persistent challenges in obtaining comprehensive information on the impact of disasters on cultural heritage, emphasizing the need for improved data collection and assessment methodologies in this critical domain, which are essential for damage model calibration and validation.

This paper focuses on the analysis of damage to CH assets as a consequence of a flood event. First, an ex ante analysis was performed using the available data. The official existing hydraulic hazard maps and the national CH database were considered. However, the pivotal aspect of this study lies in the ex post damage assessment. A well-defined workflow has been proposed to assess the tangible and intangible losses incurred by CH due to flooding: (i) identification of the assets potentially damaged by the flood, (ii) field data collection for the assessment of damage to CH, (iii) ex post damage assessment considering both tangible and intangible values of the damaged assets, and (iv) analysis of the possible contributing factor of the damage to CH.

The proposed method is applied to the case study of the flood event that impacted the Marche region (central Italy) on 15–16 September 2022. The involved sites encompass different types of assets such as churches, historic bridges, and industrial buildings, which are located in three basins in the Marche region: Burano, Cesano, and Misa.

With the method proposed in this paper, we aim to fill the gap in the literature concerning ex post assessment of cultural heritage damage induced by floods. The research pinpoints the factors that significantly contribute to the vulnerability of cultural heritage and the resulting flood-related damage.

2   Materials and methods

This section outlines the evaluation of flood damage to CH assets using two approaches: ex ante and ex post. Section 2.1 details the ex ante damage analysis, which was conducted using available data. On the other hand, Sect. 2.2, the focus of the paper, describes the procedure for the ex post damage assessment.

2.1   Ex ante damage assessment

The aim of the ex ante damage assessment is to investigate if using the available data before the flood event, it would have been possible to predict the degree of flood damage to CH. The database of CH considered for this analysis consists of the assets included in the national Italian Ministry of Culture (MIC) database (Istituto Superiore per la Conservazione ed il Restauro, 2024). The database contains movable and immovable assets under protection with declared cultural interest of national level of listing as well as UNESCO sites. In addition, it includes assets older than 50 or 70 years under evaluation to verify their effective cultural interest (D.lgs. 22 gennaio 2004, 2004). The assets that overlap with the official map of flood hazard areas are then considered. The ex ante damage assessment was evaluated as the combination of exposure and vulnerability (Arrighi et al., 2023b).

Exposure of CH can be evaluated by intersecting the shapefile of CH with the official flood hazard map available from the website of the competent authority (AUBAC, 2024). As the MIC database does not provide information about CH value and assets of regional or local listing are not included, an exposure score equal to 1 ($E = 1$) is assigned to all assets that overlay areas with some probability of inundation (i.e. P3 – high probability; P2 – medium probability; P1 – low probability). On the other hand, a 0 score is attributed to all those assets that are not potentially flooded.

According to the vulnerability classification of Arrighi et al. (2023b), a vulnerability class is defined for each CH based on its typology:

- very high vulnerability, which includes religious, residential, tertiary, and fortified architectures, as well as museums;

- high vulnerability, which includes industrial, productive, and rural architectures, as well as monuments;

- medium vulnerability, which includes archaeological areas, infrastructure, and plants;

- low vulnerability, which includes open spaces.

According to this approach and based on the available data, considering the same value ($E = 1$) for all assets then results in damage equal to vulnerability.

2.2   Ex post damage assessment: the workflow

The proposed workflow consists of four steps. The first step is focused on the identification of CH assets actually damaged by the flood (Sect. 2.2.1). Then, in the second step, a post-event field survey, based on on-site visual inspection, is conducted to evaluate the actual state and condition of CH assets (Sect. 2.2.2). Once all the data and information on the damage to CH assets are obtained, the ex post evaluation can be carried out assigning the intangible value to the assets, as well as the tangible and intangible losses based on post-event evidence (Sect. 2.2.3). Lastly, the analysis of which factors contributed most to the damage, by means of geospatial methods, is performed (Sect. 2.2.4).

2.2.1   Identification of CH assets potentially damaged by the flood

The initial step is dedicated to identifying CH assets situated within the flooded areas. For the purpose of this paper, CH refers to immovable and movable assets that hold aesthetic, historical, testimonial, municipal, and touristic value. The MIC database is considered the source for identifying CH assets that reflect this definition. The data can be downloaded from the MIC cartographic tool (Istituto Superiore per la Conservazione ed il Restauro, 2024), which comprehends architectural and archaeological assets, as point features. After the field survey verification, the list of the assets included in the MIC database could be modified, possibly adding and also disregarding some assets, as explained in Sect. 2.2.2. Once the database of CH is obtained, the identification of the assets potentially damaged by the flood is accomplished through the availability of the map of flooded areas (shapefile format) that is freely available for download from COPERNICUS (Emergency Management Service – Mapping, 2022). The flood map generation is based on the acquisition, processing, and analysis, in rapid mode, of satellite imagery and other geospatial raster and vector data sources. The identification of potentially damaged assets is obtained by overlaying the shapefiles of the flooded area and the CH database in a GIS environment. In this way, it is possible to obtain a database of CH assets affected by a flood event, which contains key information, such as name, type, and geolocalization of each individuated asset.

2.2.2   Post-event field data collection

As mentioned in Sect. 2.2.1, the list of damaged CH was updated after the post-event field data collection. Additional assets not included in the MIC database but identified as culturally significant by local authorities were considered for the ex post damage assessment. On the other hand, the assets listed in the MIC database that are not mentioned by local authorities and by official tourism websites or have no reviews on major platforms (e.g. Tripadvisor and Google) could be ex-

cluded. Indeed, as described in Sect. 2.1, the MIC database also includes assets older than 70 years, pending verification of their cultural significance. Consequently, the database may contain many private houses or industrial structures older than 70 years old that lack cultural significance or tourist interest. However, the completeness of the damaged CH assets was reviewed in collaboration with local authorities.

A novel procedure for data collection aimed at assessing the damage to CH as a result of flooding has been conceptualized. The data collection forms implemented by Molinari et al. (2014) for residential buildings and industrial facilities were modified and adapted to the characteristics of CH. Besides the information about the asset, the flood event (e.g. maximum water level), the presence and typology of any movable artworks, and the observed physical damage, the form allows for the registration of the cultural value of the CH. Table 1 summarizes the information collected on the field, through the survey form.

Among the most significant values to be measured in the post-event field survey are "h_g", "Δq", "MWL", and "mwl" (diagram in Table 1). The h_g value represents the elevation of the construction, such as the height of the steps leading into a religious building. The term Δq indicates the difference in elevation between the ground level outside the considered CH asset and a reference point in a flat area. MWL and mwl indicate the maximum water level outside and inside the construction, respectively. Concerning the mwl, it could be very different from the MWL depending on variations in h_g.

When a flooded CH site can be clearly geolocated, it may be sufficient to measure the MWL from the ground floor where the asset is located to the mud marks that were still visible at the time of the field survey. If variations in the MWL are observed around the perimeter of the structure, multiple measurement points should be recorded, and an average height value can then be calculated. This measurement can be done using a traditional meter or a laser distance meter. In cases where accurate geolocalization of the CH site is not feasible due to a lack of detailed topographic maps or databases or if the asset is located on uneven terrain with significant elevation changes, a suitable reference point should be selected. This reference point should be in a flat area whose coordinates can be easily identifiable on a GIS system. Therefore, the Δq (diagram of Table 1) can be measured. By adding Δq to the MWL, the maximum water height can then be accurately mapped within a GIS system. Practically, an operator, using a laser distance meter, points horizontally from the measurement level to the reference level, while another field operator located on the reference point can measure the height of the laser from the ground level.

In the case of a levelled bridge, the reference level from which the MWL is measured corresponds to the deck. In contrast, for a downward-arched bridge, the reference level should correspond to the intrados, and for an upward-arched bridge, it should correspond to the extrados.

As concerns the cultural value assignment, the following procedure is adopted. Based on the qualitative descriptors introduced by Historic England (2008), non-extractive and non-use values were outlined in four categories: evidential, historical, aesthetic, and communal value:

- Aesthetic value includes aspects of sensory and intellectual stimulation from the CH.

- Historical value derives from the connection between the past and the present through the asset. It includes (i) an illustrative value if the asset illustrates something unique or rare and (ii) an associative value if it is associated with a notable family, person, or event.

- Evidential value derives from the potential of the asset to yield evidence about past human activity.

- Communal value derives from the meanings of a place for the people who relate to it or for whom it figures in their collective experience or memory. It encompasses (i) commemorative value, (ii) social value, and (iii) spiritual value.

Each category of value can be described by four qualitative levels ranging from unknown or no value to high value: the respective "V" score was assigned to each asset. It is noteworthy that the chosen hierarchical system incorporates "unknown value" and "no value" levels. Indeed, in case of scarce data, it could be challenging to distinguish between sites that lack certain categories of value and assets whose value in those categories is unknown. Table 2 summarizes, for each category of value, the criteria to be considered when assessing the level of value of the cultural property and the scores corresponding to each class of value.

Following Romão and Paupério (2021), the baseline predisaster intangible value (BV) of a certain CH asset will then correspond to the sum of the scores established for each type of value given by

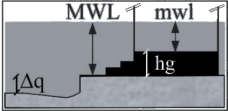$$\text{BV} = \sum_{i=1}^{4} V_i, \tag{1}$$

where V_i is the score of the typologies of value.

While Romão and Paupério (2021) proposed six classes based also on the level of interest of the asset, the classification proposed in this paper required a simplified classification with four value categories. Indeed, the available information does not allow for a more detailed assignment of intangible value classes. Therefore, the scores assigned to the class value are independent of the level of listing/protection of the CH assets.

2.2.3 Ex post damage assessment

The level of damage is obtained by combining loss in tangible and in intangible values. Loss in tangible value is strictly

Table 1. Survey form: description of CH assets and aspects considered.

Form type	CH/flood/damage description	Aspects
General information		
	General features of CH	Geographic coordinates or address
		CH denomination
		Level of listing
		Typology of CH
		Current use
		Cultural value
		Property
		Fieldworker
	Construction features	Period of construction
		Type of structure
		External ornamental elements
		No. of floors and construction height
		Presence of basement floors
		Height of the inside ground floor (h_g)
		Height difference between CH and a flat area (Δq)
	Flood characteristics	Duration
		MWL
		mwl
		Sediments grain size or contaminants
	Identification and type of damage	Structural, loss of accessibility
		Features damaged
Construction internal damage		
	Damage to floors (exposure/vulnerability of the containing construction)	Covered and uncovered surface
		Level of maintenance
		Presence and type of plants
		Damage to frescoes and wall paintings, doors and windows, floors, plants
Content damage		
	Identification of movable assets	Presence and type of artworks
	Damage to the artworks (exposure/vulnerability of contents)	Damage to furniture, paintings, sculptures, books, decorative items, votive and liturgical elements, textile, archaeological finds

linked to the observed physical damage caused by the flood. It includes structural and non-structural damage. The Italian Civil Protection Department defines structural damage as that involving the load-bearing elements of s building, such as walls, arches, pillars, beams, and slabs. In the case of non-structural damage, the elements that do not affect the stability of the building such as ceiling and floor finishes, plumbing, and electrical systems are affected.

Concerning the loss in intangible value, this is mainly caused by the direct impact of floods, as well as by indirect impacts such as mould and moisture, albeit in a less impactful way. Loss in aesthetic value refers to the effectiveness of restoration in allowing the community to be sensorially stimulated by the asset again. The impact on historical and evidential values depends on how the flood impacted the original structure and materials or the proof of past human activities, such as plaques or archives. Finally, the loss in communal value is measurable as the duration of inaccessibility of the asset (Historic England, 2008). In general, physical damage can lead to a loss of aesthetic value, and if the damage includes the complete destruction of the site, it will result in a total or near-total loss of historical and evidential value. In this paper, we assume that an asset sustaining moderate damage may be closed for days or weeks for clean-up and safety check operations, whereas an asset with severe damage may be closed for months for restoration works. It is also assumed

Table 2. Classification and criteria to define intangible value of CH with their respective class and associated score.

Type of value	Criteria to assign CH value	Class value and score (V_i)
Aesthetic	Valuable structure (e.g. architectural art using local materials or high-value import materials) and valuable artworks inside (objects of outstanding artistic quality, precious votive elements)	High (10)
	Valuable structure or valuable artworks	Moderate (7)
	No uncommonly attractive qualities but that display particular characteristics of an identified style	Limited (3)
	No valuable characteristics or stylistic features	Unknown or no value (0)
Historical	Proved illustrative and associative value or pre-19th-century structure	High (10)
	19th-century structure	Moderate (7)
	Early-20th-century structure	Limited (3)
	Late-20th-century structure	Unknown or no value (0)
Evidential	Physical remains of past human activities. The current use has not deleted proof of the past.	High (10)
	No evidence of the past, but their history is based on past human activity.	Moderate (7)
	Only the denomination recalls past human activity.	Limited (3)
	Not linked to past human activities	Unknown or no value (0)
Communal	Spiritual, social, or commemorative value. Additionally, committees have been founded to promote or defend the asset, or the asset is linked to a specific local tradition.	High (10)
	Spiritual, social, or commemorative value. No committees or traditional events are linked to the asset.	Moderate (7)
	Limited spiritual value (e.g. place of worship with sporadic openings). No traditional events are linked to the CH.	Limited (3)
	No spiritual, social, or commemorative value	Unknown or no value (0)

that if an asset remains inaccessible for more than 1 year, the loss in intangible value is comparable to the destruction, as the community will move to a new place to express communal value.

Damage is categorized into four hierarchical classes, with each asset assigned both a loss in tangible value (LTV) and a loss in intangible value (LIV). As reported in Table 3, LTV ranges from 5 to 30. The minimum value is greater than 0 as the classification system is designed for those assets actually damaged by the flood, even if only slightly, so that cleaning is sufficient to restore them. We assumed a degree of damage that varies linearly for the first three classes: "slightly damaged" (LTV = 5), "moderately damaged" (LTV = 10), and "severely damaged" (LTV = 15). On the other hand, in the case of a "destroyed" asset (LTV = 30), the assigned score is double that of the "severely damaged" class. This emphasizes the difference between a severely damaged site that can be repaired despite the high cost and a lost site that cannot

be restored. Regarding the calculation of LIV, the methodology outlined in Romão and Paupério (2021) is applied. This method employs a coefficient D (Table 3), which spans from 0 to 1, associated with each class of loss or damage. Then, for each cultural heritage asset, the loss in LIV is defined applying Eq. (2):

$$\text{LIV} = \sum_{i=1}^{4} V_i x D_i, \tag{2}$$

where V_i represents the score of the category of values. As shown in Table 2, the score of V ranges from 0 to 10, while the coefficient D could be at most equal to 1, resulting in a LIV score that ranges from 0 to 40. This implies, therefore, that greater weight is given to LIV than to LTV to emphasize the peculiar contribution of intangible aspects to the loss evaluation. In contrast to LTV, where the first damage class starts at 5, the first class for LIV can be 0. Indeed, in cases

Table 3. Classes of damage and definition of LTV and LIV.

Classes of damage	LTV	LIV
Slightly damaged	CH can return to its original state with deep cleaning.	The intangible values have not been impacted. The site has never been closed off, but the flood has limited the accessibility to the site during the event or in the immediate aftermath.
	LTV = 5	$D = 0$
Moderately damaged	Slight structural and non-structural damage (door unhinged, appliances damaged, and presence of mould).	Restoration can repair most of the features that provide aesthetic, historic, or evidential value. The site has been closed for days or weeks.
	LTV = 10	$D = 0.3$
Severely damaged	Building and artworks damaged (wrecked floor, wall painting, sculptures, paintings, furniture, wooden choir, pipe organ, liturgical supply ruined).	Despite restoration works, the damaged features that hold aesthetic, historical, and evidential significance cannot be fully restored to their original state. The site has been closed for months.
	LTV = 15	$D = 0.7$
Destroyed/lost	Asset destroyed (the construction materials are not on site anymore).	Loss in significance. The site or its most relevant features are destroyed and/or closed for more than 1 year.
	LTV = 30	$D = 1$

where an asset is only muddied without sustaining further damage, no loss of intangible value has occurred, allowing the population to continue enjoying its values. All damage classes for LTV and LIV, along with the criteria adopted to define the loss scores, considering both tangible and intangible features, are reported in Table 3.

2.2.4 Factors influencing flood damage

Flood damage to constructions can be caused by several factors, both intrinsic, influenced by the properties of the structure itself, and extrinsic, influenced by the dynamics of the flood event. In the literature, the following factors are typically considered: intrinsic factors of the construction, such as the built material, the presence of contents susceptible to flood damage and with significant cultural value, the existence of possible water communication between the construction and the river, the presence of defence elements, age in years, number of floors, shape, orientation in respect to the water flow, state of conservation, and objects that drag the sheet of water; extrinsic factors such as maximum water level outside the construction, flow velocity, hydrodynamic pressure, flood duration, presence of sediments, and contaminations (e.g. Smith, 1994; Kreibich and Thieken, 2008; Dall'Osso et al., 2009; Dutta et al., 2011; Galasso et al., 2021; Marín-García et al., 2023).

These factors can be directly assessed by means of post-event field survey or by the interpretation of post-event pho-

tos and videos and can be classified based on the level of difficulty in obtaining them (Marín-García et al., 2023).

Additionally, other authors (e.g. Cuca and Barazzetti, 2018; Di Salvo et al., 2018; Kefi et al., 2020; Al-Kindi and Alabri, 2024) also consider some geospatial factors as they could influence construction damage: difference between the level of the ground floor of the construction and the riverbank, distance from the river, difference between the digital terrain model (DTM) and the filled DTM, local slope, curvature, topographic wetness index (Beven and Kirby, 1979), stream power index (Moore et al., 1991), terrain ruggedness index (Riley et al., 1999), and normalized difference vegetation index (NDVI).

The relationship between MWL and structural damage is well known in the literature. For its evaluation, post-event field survey measurements are necessary (as described in Sect. 2.2.2). On the other hand, the evaluation of the geospatial factors requires the use of source data in vector (e.g. hydrographic network, and constructions) and raster formats such as the digital elevation model (DEM), which are generally available from national or regional databases. Concerning the DEM spatial resolution, the degree of damage to constructions could result from small variations of the morphology. For this reason, the use of high-resolution DEMs (cell size ranging between 1×1 m and 5×5 m) is recommended, especially in the case of urban flood analysis (Mark et al., 2004; Adeyemo et al., 2008; Di Salvo et al., 2018).

Specific procedures using GIS tools are implemented to assess two factors: the minimum distance (ΔD) between a CH asset and the river and the elevation difference (ΔE) between the CH asset and the riverbed. For a more accurate evaluation of some of these factors, it is advisable to rely on the areal extent of the CH asset rather than on a single point. In this respect, GIS analysis for the analysed assets can be conducted using the polygon shapefiles of constructions, which are generally available in regional or national databases. If polygonal shapefiles are not available, the shape of the assets can be digitalized based on sufficiently detailed topographic maps or aerial photos. For ΔD, the centroid of the construction polygons is considered, with the river network as the reference for distance evaluation. Using the centroid of the constructions and the nearest point on the hydrographic network, the ΔD factor is determined automatically with GIS tools (e.g. the Near tool in Analysis Tools of ESRI^{TM} ArcGIS Pro^{TM}). Concerning ΔE, for each construction polygon, the median value of the DTM is extracted. The elevation difference between the CH asset polygon and the nearest point feature on the riverbed is then calculated. To refine the riverbed elevation, a buffer distance around the riverbed can be considered.

Concerning the river slope (RS) factor, we assume that the average slope of the riverbed is a reasonable proxy for the river flow velocity, which is difficult to estimate in the absence of instrumented sections or video recordings during a flood. Moreover, the slope of the river also influences the transport of sediment and the grain size, which in turn can affect the degree of damage. To the best of our knowledge, there are no specific recommendations for RS evaluation in the literature. In this paper, the average slope of 500 and 1000 m upstream stretch with respect to the assets is considered.

Regarding the other geospatial factors, these can be evaluated as indicated by the relevant literature cited above. To evaluate the relationship between each contributing factor and the tangible and intangible losses, the mean and median values of the area of each CH asset polygon are considered.

To explore the correlation between LTV and LIV with the contributing factors, both LTV and LIV were normalized relative to their maximum values, assigning 1 to represent maximum damage and 0 to represent minimum damage. A simple correlation analysis was then performed using a linear model (Sect. 4.1.2).

3 Case study

The method is applied to CH assets damaged by the 15–16 September 2022 flood in the Marche region. This section includes an overview of the basins, along with a general description of the municipalities and their historical significance (Sect. 3.1). Moreover, the dynamics of the intense rainfall event and associated flooding are described in Sect. 3.2.

The geospatial data utilized for the analyses outlined in Sect. 2.2 were sourced from official regional and national databases. Vector data (such as buildings and river network) and the numerical technical map of the Marche region ("CTR", scale 1 : 10 000) were obtained freely from the Marche regional cartographic data portal (REGIONE MARCHE, 2023). The lidar-derived DEM, with a spatial resolution of 1 m and vertical accuracy of 0.15 m (comprising both DSM and DTM data), was acquired following a request to the Italian Government's Ministero dell'Ambiente e della Sicurezza Energetica (MASE, 2024). Specifically for the coastal area of Senigallia, a portion of the lidar data utilized had a spatial resolution of 2 × 2 m.

3.1 Overview of the study areas

The CH assets damaged by the flood are distributed across three basins on the eastern slope of the central Apennines of the Marche region, in central Italy (Fig. 1a, and b). The basins are drained by their respective main rivers: Burano (a right tributary of the river Metauro), Cesano, and Misa (Fig. 1b). The highest peak of the study area, Monte Catria (1704 m a.s.l.), is situated at the watershed between the Burano and Cesano basins. The highest peak of the Misa basin corresponds to Monte Sassone, reaching an elevation of 826 m a.s.l. (Fig. 1b).

The CH assets damaged by the flood are included in the municipalities of Cantiano and Cagli (Burano basin), Pergola and the hamlet of Bellisio Solfare (Cesano basin), and Senigallia (Misa basin), in Pesaro–Urbino and Ancona provinces.

These localities exhibit diverse historical and cultural attributes. The historical significance of Cantiano and Cagli is notably linked to the ancient Roman road known as the Flaminia, which was inaugurated between 223 and 202 BCE (Clini et al., 2023). One noteworthy site from the Roman period along the Via Flaminia is the Ponte Grosso bridge, represented by the white dot between Cantiano and Cagli (Fig. 1b).

As for the Cesano basin, the site of Bellisio Solfare has a recent history starting from the late 1800s, with the beginning of construction of the sulfur refinery. This location holds significance as part of the Marche Mining Geopark, established in 2001 (Sulphur, 2024). Pergola, known as the "city of a hundred churches", has been inhabited since prehistory, with the cultural heritage most extensively documented originating from the Roman period.

The city of Senigallia has a rich historical background, as it was the first Roman colony to settle in the Adriatic coastal plain. In the realm of flood risk management, the origins of protective measures can be traced back to the early Roman settlements (De Donatis et al., 2019). Notably, the interventions were directed toward the construction of walls along the course of the river Misa, with the dual function of both military and flood defence of the city of Senigallia. The construction of the walls, as well as other changes to the minor
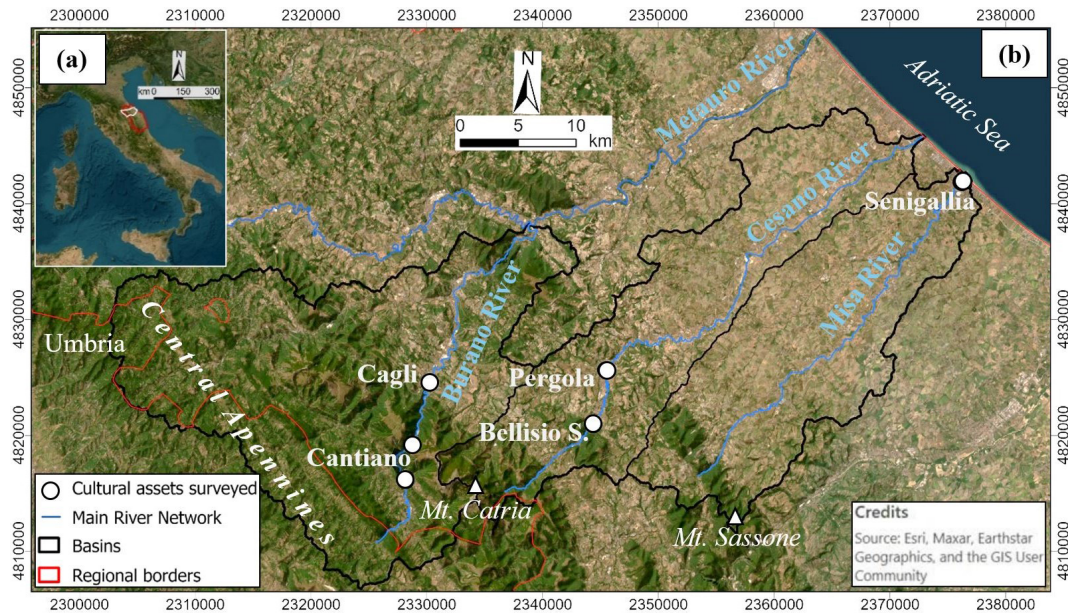
Figure 1. (a) The study area in central Italy. In red is the border of the Marche region, and in white is the area of the basins which includes the assets involved during the flood that occurred on 15–16 September 2022. **(b)** The three basins that include the assets affected by the flood: Burano, Cesano, and Misa. Coordinate system: WGS 1984 UTM zone 33N.

hydrographic network carried out by the Romans, preserved the city from flooding by the river Misa. However, during the post-Roman age, the dismantling of these walls exposed a significant portion of the city to floods, as evidenced by the event in 1472 and subsequent flooding between the 16th and 18th centuries. The aftermath of these post-Roman age flood events, combined with continuous human interventions, contributed to shaping the current topography of the urban area in Senigallia (De Donatis et al., 2012).

3.2 The 15–16 September 2022 flood event

On 15–16 September 2022, following an extended period of drought in the preceding months (Pulvirenti et al., 2023), the northern Marche region experienced very intense rainfall due to the formation of a stationary self-regenerating thunderstorm system over the Apennine Mountains, resulting in disastrous floods. From early afternoon on 15 September, rainfall started to affect the Monte Catria area, until it also extended to the mountainous areas of the Burano, Cesano, and Misa basins. In Fig. 2 the rainfall and hydrometric data of the event are reported. The data were downloaded from the civil protection monitoring system website of the Marche region (SIRMIP ON-LINE, 2024) and then elaborated on.

The most intense phase of the event occurred between 18:00 and 19:00 LT, with maximum hourly peaks of about 100 mm recorded by stations near Monte Catria, at the watershed between Burano and Cesano basins. In the Misa basin, the maximum hourly peak was recorded at 19:30 LT, amounting to about 80 mm (Fig. 2a and b).

The map of Fig. 2c, obtained interpolating the rain gauges data using the inverse distance weight interpolation method (Shepard, 1968) in ESRI™ ArcGIS Pro™ (IDW tool in Spatial Analyst tools), highlights the high spatial variability of the rainfall event.

The rain gauges surrounding Monte Catria, at the watershed between the Burano and Cesano basins, recorded the highest hourly rainfall intensity and cumulative rainfall, reaching 420 mm in 12 h. In contrast, in the Misa basin, the maximum cumulative rainfall recorded northeast of Monte Sassone is half the amount of the rainfall in the Monte Catria area. In just 6 h, about half the precipitation that typically occurs on average in a year (i.e. 780 mm, REGIONE MARCHE, 2021) fell in the mountainous areas of the Burano, Cesano, and Misa basins. A return period of > 1000 years has been estimated for rainfall durations of 3, 6, 12 and 24 h at the rain gauges located in areas characterized by higher rainfall intensities (REGIONE MARCHE, 2022).

Although about half as much rain fell in the Misa basin as in the Burano and Cesano basins, the effects were still disastrous. One reason can be attributed to the different geology of the basins (e.g. Iacobucci et al., 2022). The Monte Catria ridge in the Burano and Cesano basins mainly consists of fractured carbonate rocks, which contribute to the infiltration processes (Mastrorillo and Petitta, 2014), mitigating flood effects. On the other hand, the Misa basin is mainly composed of clays and sandstones, which are less permeable. As a result, a larger portion of the rainfall contributed to runoff processes, exacerbating flood dynamics.
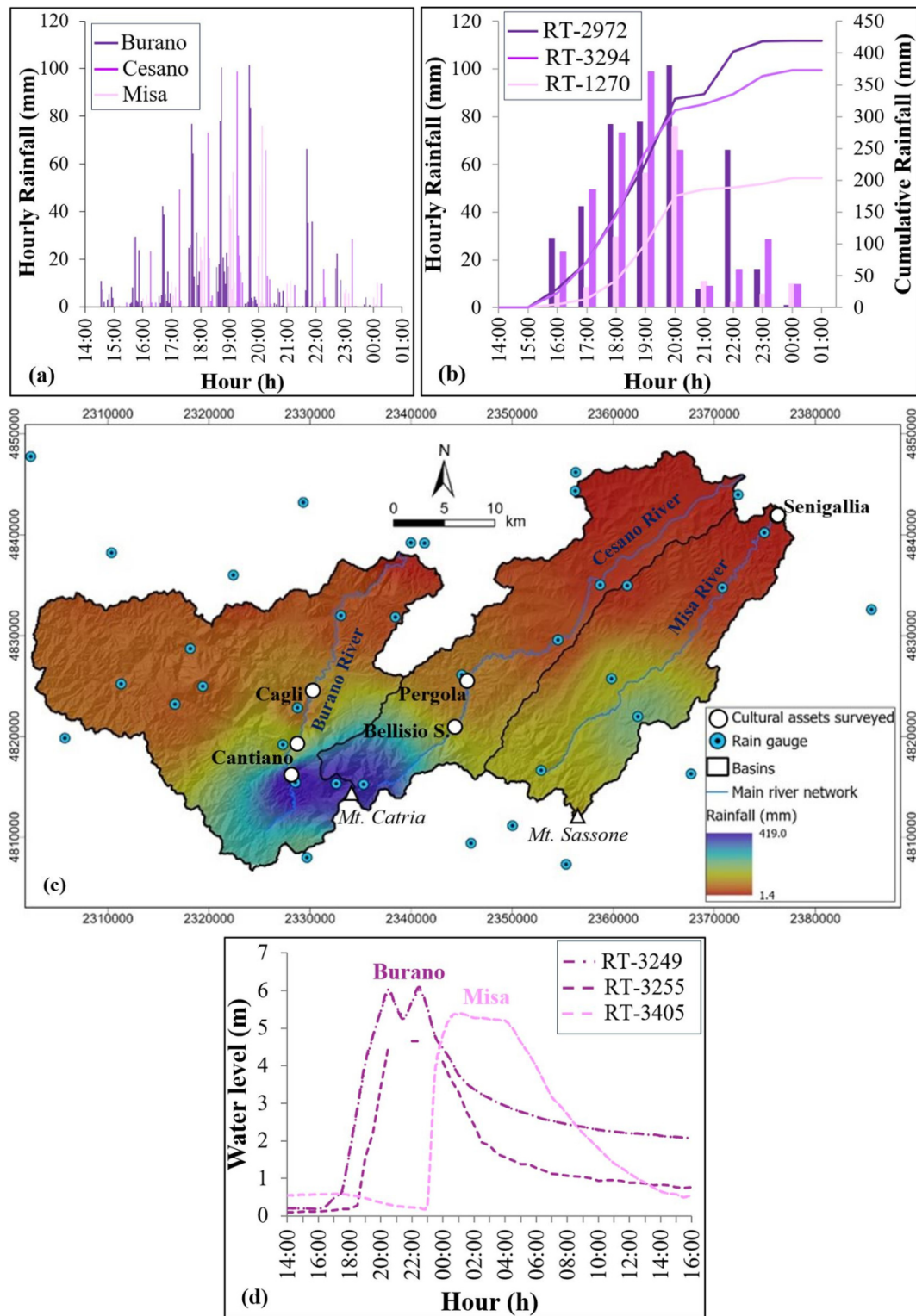
Figure 2. Observed rainfall and flow rate of the 15–16 September 2022 event. **(a)** Hourly rainfall measured by the rain gauges in the three basins, **(b)** the three rain gauges of each basin that measured the maximum cumulative rainfall, **(c)** map of the cumulative rainfall, and **(d)** measured water level by a hydrometer of the river Burano and river Misa. Rain gauges codes: Cantiano RT-2972 (Burano basin), Monte Acuto RT-3294 (Cesano basin), and Colle RT-1270 (Misa basin). Hydrometer codes: Pontedazzo RT-3249 (1 km downstream Cantiano, river Burano), Cagli Ponte Cavour RT-3255 (river Burano), and Ponte Garibaldi RT-3405 (Senigallia, river Misa). The shaded relief basemap of panel **(c)** was obtained from the TINITALY DEM (Tarquini et al., 2007, 2023). Distributed under the CC BY 4.0 license. Coordinate system: WGS 1984 UTM zone 33N.

The hydrometers reported in Fig. 2d, in the Burano basin, are located in the Pontedazzo section, which is 1 km downstream from Cantiano (RT-3249), and in Cagli (RT-3255). The intense rainfall that fell over a brief period led to an abrupt increase in the river discharge, as highlighted by the water level variations of the Burano and Misa rivers (Fig. 2d). The blockage of bridges and culverted stretches significantly contributed to the flooding. In Cantiano, the flooding of the urban centre occurred from the culverted section of the river Burano, as shown in some videos recorded by residents (e.g. World Events News, 2022). In the case of Senigallia, a video shows the evolution of the flooding of the river Misa (Storm Chasers Marche, 2022). In this case, large woody debris crashed against the deck of the bridges Corso 2 Giugno and Garibaldi (where the hydrometer is located), causing widespread flooding throughout the city.

A total of 13 people died, and severe damage resulted in most settlements along the main rivers. Further details on flood dynamics in Cantiano, Cagli, Pergola, and Senigallia, as well as the consequent damage to CH assets, are provided in Sect. 4.2 of the results.

4   Results and discussion

The results of applying the proposed method to assess the damage to CH assets caused by the flood event that occurred on 15–16 September 2022, in the Burano, Cesano, and Misa basins, are presented and discussed in two main sections. Section 4.1 concerns the analysis of the results obtained by applying the ex post damage assessment method, which is the main goal of this paper. In Sect. 4.2 the results of the ex ante application are compared with the ex post results and then discussed. The shapefile of the collected data and the ex post damage assessment form are provided in the "Data availability" section of this paper.

4.1   Ex post damage assessment

4.1.1   Features of the CH assets and losses assessment

Remote analysis and field survey verification ensure the identification of all the CH assets actually damaged by the flood. A total of 14 assets were identified, for which maximum water level (MWL), baseline value (BV), and both losses in intangible (LIV) and tangible (LTV) scores are provided in Table 4. Most of the damaged CH assets are religious building types (6 out of 14), while the remaining damaged assets include bridges, a fortified gate, a square, a porch, and residential or industrial architecture. Among the 14 assets identified, 3 of them (Ponte Garibaldi, Sant'Emidio Oratory, and Santa Maria del Porto Church) were not present in the MIC database and were therefore added as CH assets during the field survey, according to the local authorities. Based on the suggestions of local authorities, even sites absent from the MIC database should be considered of national significance,

as they meet the criteria defined by national cultural heritage laws. Therefore, the listing level for all 14 assets damaged by the 2022 Marche flood is classified as national.

Figure 3a shows the general view of the basins, and Fig. 3b–g highlight the distribution of the BV and LIV scores for the sites of the three basins. Figure 4b–g report the distribution of the LTV scores throughout the basins; panels h and i depict how the MWL was estimated during the field survey, in the case of a generic building and a bridge, respectively; in panels b1–c2 two post-event photos showing the MWL are reported. In panels b–g of Figs. 3 and 4, the labelled CH asset points correspond to the centroids of the polygon shapefile of the Marche regional cartographic data portal (REGIONE MARCHE, 2023). In the cases of the Sant'Emidio Oratory and the two bridges Ponte Grosso and Ponte Garibaldi, the polygonal shapefile of these assets was missing. Hence, their shape was digitized based on the topographic map, and the centroid was extracted accordingly (as described in Sect. 2.2.4).

The most valuable cultural asset corresponds to the Santa Maria delle Tinte Church (BV = 37), which is located in Pergola, within the Cesano basin (Fig. 3e, label 7). The maximum aesthetic, historical, and communal values are assigned to that asset, as the church was adorned with statues and stucco decorations, in addition to precious 18th-century wooden pews, painted with floral motifs. Moreover, the church was built at the behest of the historical dyers and wool merchant guild, and still today it is a representative place in the city. Indeed, after the 2022 flood, a committee called Gli Angeli delle Tinte was assembled to propose a restoration project for the church (FAI, 2022). In general, religious architectures were built before the 19th century, and, in addition to the high spiritual value, valuable structures and valuable artworks coexist, resulting in a high aesthetic value. For these reasons, the average intangible value score of the damaged churches is relatively high (BV = 26), in contrast with the average score of the other asset types (BV = 18).

Ponte Garibaldi (Fig. 3g, label 13), namely the damaged bridge in Senigallia (Misa basin), has the lowest intangible value (BV = 6) for its limited historical value (it dates to the early 20th century), as well as for its limited aesthetic value. Indeed, even if it is an example of the typical early-20th-century architectural style, it is not a valuable structure. On the other hand, the other damaged bridge in the Burano basin, Ponte Grosso in Cantiano (Fig. 3c, label 2), is characterized by a higher intangible value (BV = 23). In this case, even if its aesthetic value is limited, both the historical and evidential values are high, because it is a rare example of infrastructure of the ancient Roman Empire.

It is worth noting that the Bellisio Solfare refinery asset (Fig. 3f, label 8), despite being mostly unknown among the most important tourist attractions and with a poor state of conservation, is characterized by high intangible value (BV = 27). Indeed, it represented an important proof of the past industrial activity of the Pergola municipality area (Bu-
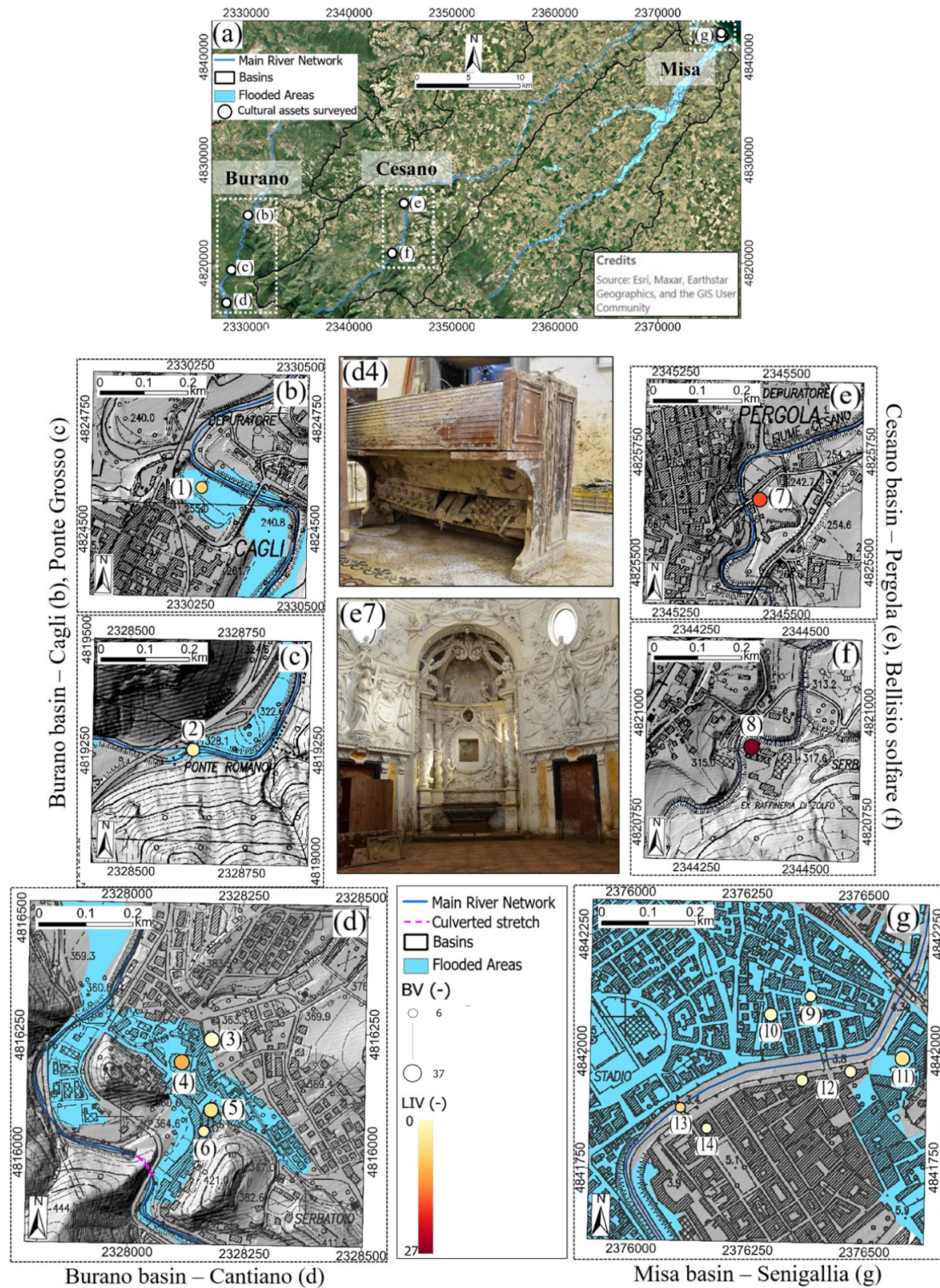
Figure 3. (a) General view of the CH assets surveyed for each basin and **(b–g)** the panels including numbered labels (1–12) representing the CH asset points showing the BV (bubble size range represents $6 \leq \text{BV} \leq 37$) and LIV (scale colours) scores of the assets. Burano basin: **(b)** Sant'Emidio Oratory in Cagli (1), **(c)** Ponte Grosso in Cantiano (2), and **(d)** the assets in Cantiano (3–6). Cesano basin: **(e)** Santa Maria delle Tinte Church (7) and **(f)** Bellisio Solfare (8). Misa basin: **(g)** the assets in Senigallia (9–14). Panels **(d4)** and **(e7)** report post-event photos of San Giovanni Battista Collegiate and Santa Maria delle Tinte Church, where damage as a result of mud deposition inside the buildings is visible. The shaded relief basemap of panels **(b)**–**(g)** was obtained from the DTM lidar of the Ministero dell'Ambiente e della Sicurezza Energetica (MASE, 2024). The numerical technical map of panels **(b)**–**(g)** is from the Marche region (REGIONE MARCHE, 2023). Both maps are distributed under the CC BY 4.0 license. Coordinate system: WGS 1984 UTM zone 33N.
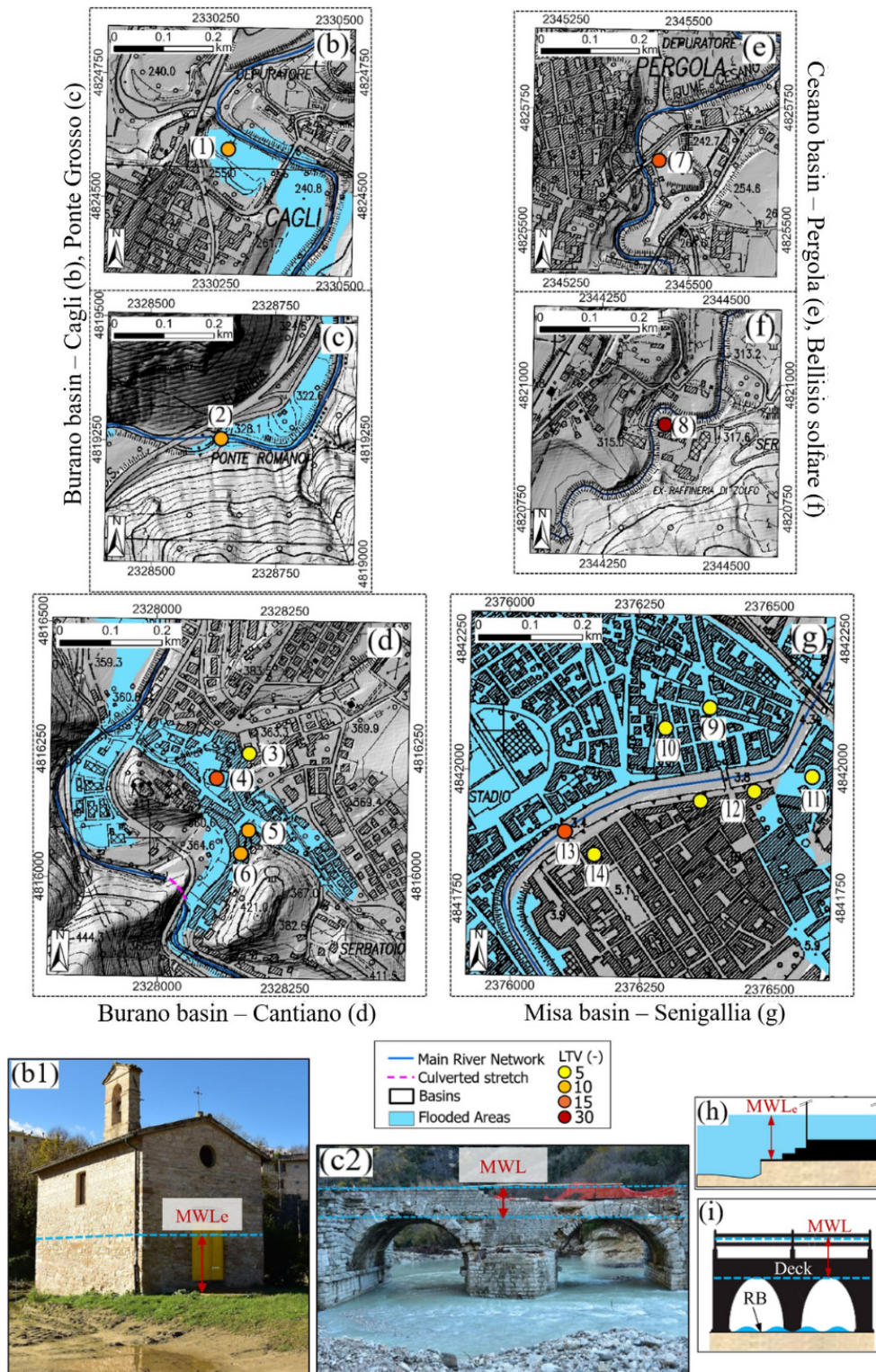
Figure 4. (b–i) The panels of the LTV scores of the assets (labels 1–12). Panels **(b1)** and **(c2)** display the post-event field survey photos depicting the damage to the Sant'Emidio Oratory and Ponte Grosso, respectively. Panels **(h)** and **(i)** report the schematic view of the MWL estimation in the case of a generic building and a bridge, respectively (RB is the riverbed). The shaded relief basemap of panels **(b)**–**(g)** was obtained from the DTM lidar of the Ministero dell'Ambiente e della Sicurezza Energetica (MASE, 2024). The numerical technical map of panels **(b)**–**(g)** is from the Marche region (REGIONE MARCHE, 2023). Both maps are distributed under the CC BY 4.0 license. Coordinate system: WGS 1984 UTM zone 33N.

Table 4. CH assets damaged by the flood, classified by basin, type, MWL, and the associated scores of BV, LIV, and LTV. Can: Cantiano; Cag: Cagli; P: Pergola; BS: Bellisio Solfare. All the assets in the Misa basin are located in Senigallia (the numbers in brackets correspond to the labels in the panels of Figs. 3 and 4).

Basins	CH assets	Type	MWL (m)	BV (–)	LIV (–)	LTV (–)
Burano	(1) Sant'Emidio Oratory (Cag)	Church	2.40	20	7	10
	(2) Ponte Grosso (Can)	Bridge	2.50	23	2.1	10
	(3) Sant'Agostino Church (Can)	Church	0.35	27	0	5
	(4) San Giovanni Battista Collegiate (Can)	Church	1.40	27	13	15
	(5) San Nicolò Church (Can)	Church	2.05	24	5.1	10
	(6) Historical buildings Via Fiorucci (Can)	House	2.30	17	2.1	10
Cesano	(7) Santa Maria delle Tinte Church (P)	Church	3.40	37	20	15
	(8) Bellisio Solfare refinery (BS)	Factory	2.66	27	27	30
Misa	(9) Porta Lambertina	Fortified gate	0.44	17	0	5
	(10) Santa Maria del Porto Church	Church	0.06	21	0	5
	(11) Foro Annonario	Square	0.65	24	3	5
	(12) Portici Ercolani	Porch	1.50	17	0	5
	(13) Ponte Garibaldi	Bridge	2.18	6	6	15
	(14) Filanda Serica	Factory	0.23	10	0	5

rano basin). Furthermore, a high communal value is assigned to it, due to the presence of an organization that aims to rebuild the asset.

The assets of historical buildings Via Fiorucci (Fig. 3d, label 6) and Porta Lambertina (Fig. 3g, label 9) are distinguished by their high historical significance, being notable architectures of the past and holding a moderate aesthetic appeal, resulting in a BV = 17. In contrast, Foro Annonario (Fig. 3g, label 11) and Portici Ercolani (Fig. 3g, label 12) are CH open spaces of notable value, with BV = 24 and 17, respectively. While these two assets share similar evaluations across most value types, the Foro Annonario holds significant community value. Indeed, it represents the historical central marketplace of Senigallia, thus remaining a vital meeting point for the city since its realization.

Moreover, Fig. 3a–g reports the extension of the flooded area from the COPERNICUS agency. In general, these maps agree with those actually flooded as a result of the event (the same for Fig. 4). The only exceptions are the areas of Pergola and Bellisio Solfare, as well as assets 12 and 14 in Senigallia. This demonstrates that these maps are useful for rapid identification of flooded areas. However, a direct field evaluation to establish which assets were effectively flooded is fundamental.

In Fig. 4–g showing the spatial distribution of the LTV scores of each asset are reported. Concerning the Bellisio Solfare refinery (Fig. 4f, label 8), the highest LIV and LTV were assigned as the flood completely destroyed the building, and during the survey, only ruins were observed (LIV = 27 and LTV = 30). The historic Santa Maria delle Tinte Church (Fig. 4e, label 7) sustained considerable damage caused by the flood, both in terms of damage to intangible and tangible

value (LIV = 20 and LTV = 15). The inundation resulted in harm to the electricity system and the emergence of mould on both the floor and wall paintings. Additionally, the force of the floodwater partially wrecked the door and destroyed the 18th-century pews. As a result, the aesthetic value of the church was deemed lost. Moreover, its extended closure period led to a significant impact on its communal value. Even the San Giovanni Battista Collegiate (Fig. 4d, label 4) experienced severe damage (LIV = 13 and LTV = 15). In addition to the effects already observed for the other assets, floor tiles were broken, the wooden choir and altars were swollen due to the floodwater, and the 16th-century liturgical supply was covered by mud. In the case of San Nicolò Church (Fig. 4d, label 5), part of the floor collapsed, and the external stone and metal balustrade were swept away by the flowing water (LIV = 5.1 and LTV = 10). Similar loss scores were observed for the Sant'Emidio Oratory (Fig. 4b, label 1), in which, however, a significant loss was due to the wooden door, as it was swept away.

Overall, a high level of losses was observed for most of the affected religious structures, where closure due to extensive damage contributed to a decrease in communal value. Conversely, the Sant'Agostino (Fig. 4d, label 3), Porta Lambertina, Santa Maria del Porto, Portici Ercolani, and Filanda Serica assets (Fig. 4g, labels 9, 10, 12, and 14) incurred the lowest losses, both in intangible and tangible aspects (LIV = 0 and LTV = 5). Specifically, the two churches were not damaged as they are over-elevated from the ground floor. For all these assets, only mud marks dirtied the external walls.

As regards the Foro Annonario (Fig. 4g, label 11), the only damage is related to the mud marks along the porch perime-

ter. Nevertheless, the relative LIV is higher than 0 (LIV = 3) since the circular square in which the porches are located remained impracticable for some days.

The two affected bridges were significantly damaged as the maximum level reached by the water during the flood exceeded the height of the deck. Portions of the arch stones of the Ponte Grosso (Fig. 4c, label 2) collapsed, leading to a moderate decrease in tangible value (LTV = 10). However, the historical and evidential aspects remained unscathed, resulting in a relatively low decline in intangible value (LIV = 2.1). Conversely, Ponte Garibaldi (Fig. 4g, label 13) sustained severe structural damage (LTV = 15). Indeed, some months after the field survey, it ultimately had to be demolished (ANSA, 2023), resulting in the loss of aesthetic and historical significance (LIV = 6).

Regarding the MWL estimate (Fig. 4, panels h and i), it was directly measured during the field survey, as detailed in Sect. 2.2.2. However, there were exceptions with the two bridges and the Bellisio Solfare refinery. Direct measurements were not possible in these instances due to the inaccessibility of the bridges, compounded by the destruction of the Bellisio Solfare asset. Consequently, for these cases, the estimation of MWL was conducted indirectly. As for the Ponte Grosso (Fig. 4c, label 2), the MWL was estimated considering wood deposition height at road signals close to the bridge (e.g. video from TGCOM24, 2022). The resulting estimated MWL from the deck is 2.5 m. With regards to Ponte Garibaldi (Fig. 4g, label 13), the highest water level value from the riverbed was recorded during the flood peak by the hydrometer on the river Misa (i.e. 5.39 m as reported in Fig. 2d). The height from the riverbed to the base of the deck was estimated, and this value was subtracted from the maximum height measured by the hydrometer, resulting in a MWL of 2.18 m. In the case of the Bellisio Solfare asset (Fig. 4f, label 8), the MWL was estimated by considering the mud marks height at the closest building on the hydrographic left of the river Cesano. The measured MWL at this building, used as a reference, is 1.45 m. Thus, considering the DTM difference between the refinery and this site, the resulting MWL at Bellisio Solfare is equal to 2.66 m.

Moreover, as the cultural assets listed in Table 4 are mostly located on flat areas, the measured Δq, as defined in Sect. 2.2.2, is negligible.

4.1.2 Factors influencing flood damage

In this study, the following factors were considered as those that can potentially contribute to the damage to CH assets: maximum water level outside the construction (MWL), maximum water level inside the construction (mwl), minimum distance between asset and river (ΔD), difference between the elevation of CH asset and the elevation of the riverbed (ΔE), difference between DTM and filled DTM (ΔDTM), average slope of the river (RS), local slope (LS),

curvature (CU), topographic wetness index (TWI), and terrain ruggedness index (TRI).

The procedures described in Sect. 2.2.2 allowed us to investigate which factors contributed significantly to both the LTV and LIV of the CH assets. Considering the mwl and h_g parameters, as they were only available for a few assets, they were not included in the damage inference analysis. Among all the factors analysed, RS, MWL, and ΔE showed some correlation to LTV (Fig. 5a–c), while for all other contributing factors the correlation proved to be negligible. The same trend also resulted in a correlation of the LIV with the same contributing factors (Fig. 5d and e). This can be explained as the LIV is linked to the LTV. Indeed, if an asset is destroyed, all the intangible values are lost too. Overall, there is a greater correlation between LTV and contributing factors than LIV, as the aspects that are not strictly related to physical parameters are considered when assessing LIV.

The factors RS and LTV (Fig. 5a), considering the 500 m stretch upstream of the single asset of a group of assets (RS500), exhibit both a higher correlation and a lower dispersion ($R^2 = 0.91$, RMSE = 0.12). Also considering the 1000 m stretch upstream from the CH (RS1000), the LTV–RS relationship is clear, although it results in a lower correlation and greater dispersion ($R^2 = 0.75$, RMSE = 0.15) than considering the RS500 factor. These results show that an increase in RS corresponds to an increase in LTV. Both 500 and 1000 m were considered as there are no clear recommendations in the literature on whether the flow of a river adapts to the slope of the riverbed. Nevertheless, considering these distances, it is reasonable to assume that the slope of the riverbed affects the energy of the flowing water and thus can be used as a valid proxy for current velocity. As observed, the dynamics of the flood event were different throughout the basins (Sect. 3.2). In the case of the river Misa in Senigallia (RS500, $1000 = 0.001 \, \mathrm{m \, m^{-1}}$), the flooding that occurred was mainly caused by the overtopping of the two bridges present, which in turn caused a progressive and slow rise in water levels throughout the city. This scenario resulted in damage to CH primarily attributable to water stagnation and the accumulation of fine sediments (ranging from clays to sands), rather than the direct impact of hydrodynamic forces from flowing water. Indeed, for all the CH assets, the minimum LTV (5) was observed (Table 4). The only exception is the Garibaldi Bridge, which was more severely damaged (LTV = 15) as it was obstructed due to the passage of woody debris and the related pressure exerted on it. On the other hand, for the sites in the Burano and Cesano basins, a steeper slope caused greater damage due to the hydrodynamic force of the water impacting the CH assets. This is evidenced by some videos recorded at Cantiano (as described in Sect. 3.2) but especially by the destruction of the Bellisio Solfare refinery (LTV = 30). In this case, the slope of the river Cesano was sufficient to transport and deposit large amounts of floating and coarse debris, including wood, gravel, and boulders, which contributed to the destruction of the site. However, it
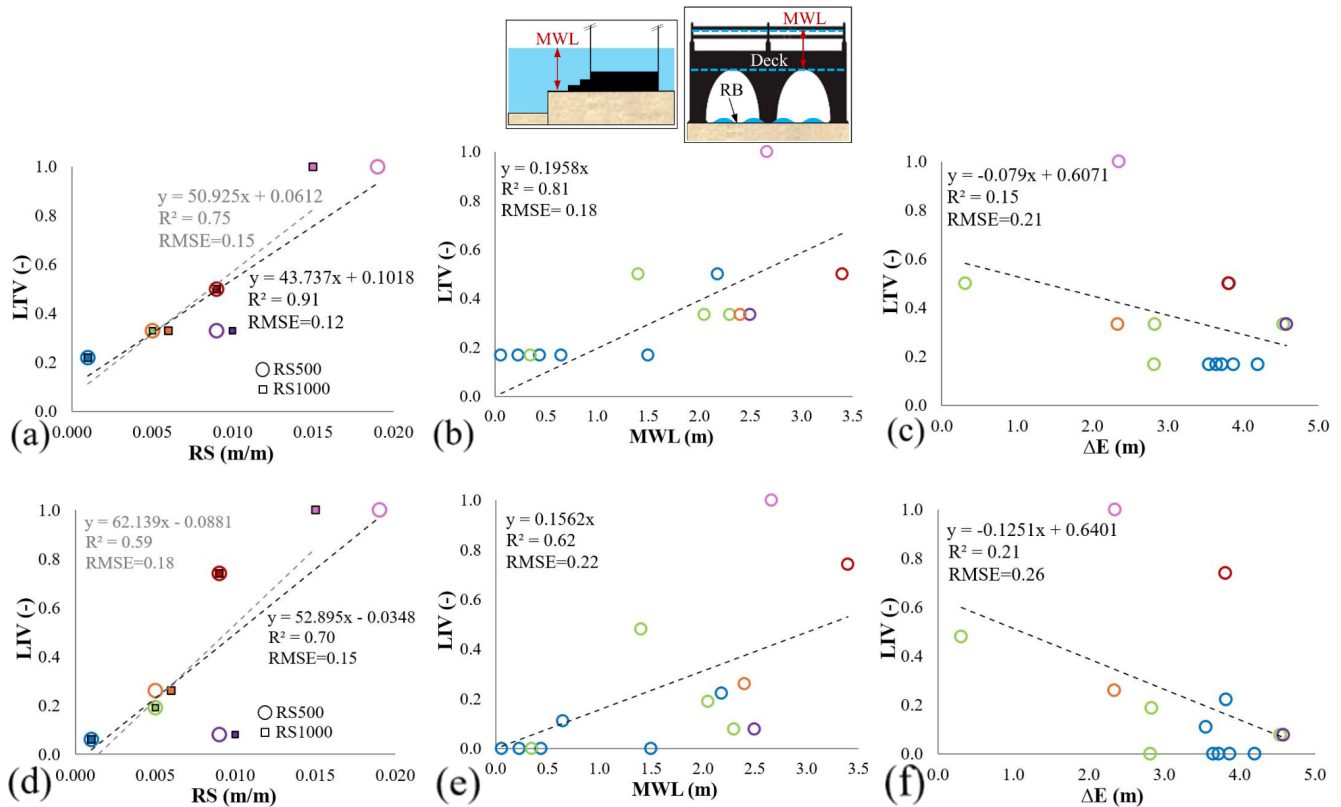
Figure 5. Relations between normalized LTV **(a–c)** and LIV **(d–f)** with influencing contributing factors: **(a, d)** RS, considering distances of 500 m (black line and circles) and 1000 m (grey line and boxes) upstream of the single asset or group of assets; **(b, e)** MWL measured as the height of the maximum water/mud mark level with respect to the outside ground floor of each asset; **(c, f)** ΔE, the elevation difference between the asset and the riverbed.

is also worth noting that this site was in a poor state of conservation, which possibly reduced structural resistance.

As concerns the correlation between LTV and MWL, Fig. 5b highlights a clear relationship. Namely, the higher the flood depth, the greater the damage is, as generally found in the literature for stage–damage functions. However, a lower correlation is observed than the LTV–RS500 relationship as well as a higher dispersion ($R^2 = 0.81$, RMSE $= 0.18$). A higher RMSE value can be justified by the Bellisio Solfare site, which represents an outlier. Indeed, the maximum assigned LTV value due to its destruction is not solely linked to the MWL but rather to the energy of the flow, as demonstrated above. The lowest correlation and the highest dispersion ($R^2 = 0.15$, RMSE $= 0.21$) correspond to the LTV–ΔE relationship (Fig. 5c).

Overall, the following results are worth highlighting:

- The correlation between LTV and LIV with ΔE is not statistically significant (p value > 0.05).

- LTV and LIV are highly correlated (Pearson's $R = 0.93$ and p value < 0.05). Despite LIV considering factors not directly related to the physical characteristics of a flood event, it still correlates well with LTV. Indeed, aes-

thetic and communal value losses are generally sensitive to flood impacts, while evidential and historical values persist despite flood damage, as the asset remains a testament to historical eras and past activities. However, if the asset is destroyed, also intangible values are lost.

- RS (i.e. a proxy for river flow velocity) is highly correlated with LTV and LIV (Pearson's $R = 0.85$ and 0.84, respectively, and p value < 0.05) but not significantly correlated with MWL (Pearson's $R = 0.62$ and p value > 0.05). Therefore, both RS and MWL are crucial for accurately estimating damage.

The obtained results are derived from specific criteria for assigning LTV and LIV scores, which rely on an expert-judgement-based quantification method. Therefore, a discussion of how correlations change considering different scores of LTV and LIV is needed. To achieve this, the analysis is conducted using scores that vary both linearly and non-linearly, categorized into four classes to ensure comparability with the approach used in this paper. Concerning the LTV, using a linear scale (LTV $= 5$–10–15–20), the relations obtained are very similar to those resulting from the scale used in this paper. Although small variations in R^2 and RMSE oc-

cur, the trends obtained are practically the same, with a high correlation with RS500 and RS1000 and very low correlation with ΔE. The largest differences occur in the case of MWL, with a significant increase in the correlation ($R^2 = 0.88$). Even using a fully non-linear scale (LTV = 5–10–20–40), the general trend remains the same, with an increase in the correlation with MWL ($R^2 = 0.75$) compared those obtained with the scale adopted in this paper. Regarding the LIV, we changed the score of V, again varying it linearly and non-linearly and using maximum and minimum values, the same as proposed in Romão and Paupério (2021). In the case of linear ($V = 0$–6.7–13.3–20) and non-linear ($V = 0$–3–12.5–20) variation, the trend is the same as those obtained in this paper, with a slightly worse correlation using a non-linear scale. Overall, varying linearly and non-linearly the scores of LTV and LIV results in trends consistent with those observed using the scales adopted in this paper. This supports the conclusion that there is a significant relationship between tangible and intangible damage and the contributing factors analysed.

As mentioned in Sect. 2.2.4, also intrinsic factors can potentially influence the damage to CH. In this regard, a relevant aspect to consider when measuring the maximum water level inside the building (mwl) and assessing the vulnerability of a CH asset, but in general of any building, is the possible presence of basements. Typically, basements increase the vulnerability of a structure to flooding, as they can lead to a higher mwl. However, it is not always the case that a higher mwl is reached at the basement level than at the upper floors. Indeed, this depends on how and whether the basement floors are hydraulically connected to the upper floors or the outside of the building. However, if the presence of the basement results in a higher water level in the basement but a lower water level on the ground flood, this could potentially reduce the observed losses. In this scenario, if the movable artworks are mostly exposed at the ground level, they may remain unaffected by the floodwater. In general, for a CH asset with several flooded floors, including the basement, it may be appropriate to measure the mwl and evaluate LTV and LIV on each floor. Then, the related average values for the entire asset can be considered for further analysis.

Moreover, also the presence of valuable contents, especially if exposed at a low level with respect to the ground floor, increases the amount of damage and therefore the restoration cost. Indeed, religious architectures that contain paintings, precious pews, and ancient elements such as organs, have incurred moderate or severe LTV, specifically the churches of Santa Maria delle Tinte, San Giovanni Battista, and San Nicolò (Table 4). On the other hand, although the Sant'Agostino and Santa Maria del Porto churches contain artworks, they have not experienced a loss in tangible value. This is attributed to their elevated positioning above ground floor level. However, it could be noteworthy that their low LTV can also be attributed to their relatively low MWL (Table 4). A more explanatory perspective on the positive impact

of elevation on damage is the San Nicolò Church. Indeed, in this case, despite a high MWL, the associated LTV is relatively low, as it is supra-elevated at 1.12 m above ground floor level (Table 4).

Even the state of conservation could influence the degree of damage. Indeed, the poor state of conservation reduced the Bellisio Solfare asset capacity to resist the impact of the water and debris mixture, contributing to its destruction. These data confirm that the degree of conservation can directly impact the extent of damage observed following a flood event (Stephenson and D'Ayala, 2014; Salazar et al., 2024).

Studies in the literature pinpoint the role of construction material in determining the vulnerability of CH assets (Balasbaneh et al., 2020; Brokerhof et al., 2023). However, no relations were found for this parameter, as all the surveyed assets are characterized by the same material (i.e. masonry structure). The only exception is the Ponte Garibaldi, which was constructed with a reinforced concrete structure.

Among the factors that have contributed significantly to the overflowing of rivers during the 2022 Marche flood event are bridges and culverts, which were clogged. In Cantiano, the inadequacy of the culverted section at the entrance of the urban area resulted in insufficient drainage of the river Burano, leading to overflow and sediment deposition. In Pergola, a bridge near the Santa Maria delle Tinte Church was blocked by sediment and woody debris, resulting in flooding of the surrounding area. In Senigallia, large woody debris blocked Ponte Garibaldi, causing the flooding of the city. It is widely observed that bridges and culverts can become clogged during intense bed load transport, hyperconcentrated flow, or debris flow events, leading to massive overflows. To mitigate the risk of clogging in complex urban environments, a river management approach that incorporates optimized design principles based on adequate field surveys, numerical modelling, and laboratory experiments is desirable (Gschnitzer et al., 2017; Amaddii et al., 2022, 2023; Martín-Vide et al., 2023; Zugliani et al., 2023). These measures would also positively impact the preservation of ancient CH assets, which are now confronted with heightened flood risks due to climate change, a risk likely lower during their construction.

4.2 Comparison between ex post and ex ante damage assessment

In this section, the results obtained through the methodology outlined in Sect. 2.1 are presented and compared to the results of the ex post damage assessment, considering only the LTV.

The first issue with the flood hazard map is its low degree of detail. Indeed, all the areas investigated are in the same class, namely medium probability (low-frequency floods), and the map lacks some useful information, such as water height or velocity. Thus, assets can only be included or excluded from floodable areas. Overlapping the assets of the

MIC database with the official map of flood hazard areas, 55 potentially damaged assets were identified. These assets were then categorized based on their typology into various damage classes: 41 are included at risk of very high damage, 6 as high, 5 as medium, and 2 as low. One of the individuated assets (Fiorentino Basso) remains unclassified due to insufficient information available in the MIC database regarding its type. Additionally, the MIC database lacks information regarding the type of value associated with each asset. It is noteworthy that only 5 in 55 identified assets are listed as damaged cultural heritage (Ponte Grosso, San Giovanni Battista Collegiate, Santa Maria delle Tinte Church, Porta Lambertina, and Foro Annonario in Table 4), based on the definition of cultural heritage given in Sect. 2.2.1. Indeed, 38 assets are residential, productive, rural, tertiary architectures, or open space that do not reflect the cultural heritage definition mentioned in Sect. 2.2.1. Consequently, no data were collected for them, and it is unknown whether they were affected by the flood. Moreover, 11 of the 55 assets are religious architectures, historical infrastructures, and open spaces with cultural interest (as defined in Sect. 2.2.1). Although these assets are located in flood hazard areas, they were not actually damaged by the flood and thus were not considered in this paper.

In addition, it should be emphasized that nine assets defy the ex ante damage assessment, even if identified as damaged during the field survey. This discrepancy arises either from their absence in the MIC database (such as Ponte Garibaldi, Sant'Emidio Oratory, and Santa Maria del Porto Church) or because they do not overlap with the flood hazard areas (including Portici Ercolani, Bellisio Solfare refinery, Filanda Serica, historical buildings Via Fiorucci, Sant'Agostino Church, and San Nicolò Church).

These findings highlight the main issues with the MIC database:

– Some assets may be inaccurately geolocalized (e.g. Bellisio Solfare refinery).

– In cases where assets have an extended area and only a small portion is potentially inundated, the point shapefile may not accurately represent their exposure, as it could be situated in unexposed areas (as observed with the historical buildings Via Fiorucci and Sant'Agostino Church). In the case of widespread assets or constructions with a linear footprint (i.e. assets including several buildings along a road or porches such as Portici Ercolani), only one centroid point representative of the location exists.

Consequently, the comparison between the ex ante and the ex post damage assessments is feasible only for five assets: Porta Lambertina, Ponte Grosso, Foro Annonario, San Giovanni Collegiate, and Santa Maria delle Tinte Church. Consistently with observations, from the ex ante damage assessment it is derived that the two churches fall into a very high

damage class, the Ponte Grosso bridge into a medium damage class, and the open space Foro Annonario into a low damage class. Observed losses thus confirm that religious architectures are the most vulnerable to flooding as assumed in most of the ex ante flood risk assessment works in the literature (Garrote et al., 2020; Arrighi et al., 2023). Porta Lambertina resulted in a high damage class, while the ex post assessment resulted in it being slightly damaged, as only mud marks were observed.

5 Conclusions

This paper developed an ex post flood damage assessment method for CH assets. This yields a semi-quantitative on-site evaluation of losses (i.e. not in monetary terms), both in terms of intangible and tangible impacts. To the best of our knowledge, it constitutes a novel aspect. The method consists of four main steps: (i) identifying CH assets potentially damaged by the flood; (ii) collecting post-event field data, through an ad hoc developed survey form; (iii) evaluating the losses in both intangible and tangible values; and (iv) analysing the factors contributing to flood damage. For step (ii), it is crucial to visit the damaged sites as soon as possible to collect data and information that may become unavailable due to restoration work. The use of the proposed form allows a quick, easy, and reproducible way for the post-event flood data evaluation to be aimed at the direct assessment of losses in intangible and tangible values of CH assets. Then, step (iii) allows us to estimate the level of losses caused by floods for both tangible and intangible values of different types of CH assets. Finally, the findings from step (iv) allow for a better understanding of the causative phenomena aimed at valuable insights for disaster risk management.

The method was applied to the CH assets damaged by the flood event that occurred on 15–16 September in the Burano, Cesano, and Misa basins (Marche region, Italy). The main findings that can be drawn from the application of the proposed method are the following:

– A post-event field survey is fundamental for gathering data and information on hazard characteristics, such as water depths, together with losses in intangible and tangible values and for subsequent analysis (e.g. GIS processing). Ex post flood damage information for CH is relevant for verifying the hypothesis of existing methods based on expert judgement. Moreover, it poses the basis for developing empirical flood vulnerability functions for CH. Peculiarities of CH, such as raised floors, presence of valuable artworks, and state of conservation are found to be relevant for flood vulnerability. Thus, where this information is not available, on-site inspections are suggested to better characterize actual exposure and vulnerability for ex ante risk analysis.

– The LTV is well correlated with the MWL, consistent with damage to other construction types. Additionally, there is also a strong correlation between LTV and the average slope of the riverbed, considering both 500 and 1000 m upstream of the assets. The slope of the riverbed, a proxy of river flow velocity, can thus be considered as one of the possible contributing damage factors (as the measured or estimated data of water velocity is difficult to obtain).

– The LIV correlates well to the same contributing factors. However, LIV data show a lower R^2 and a larger spread, demonstrating that intangible aspects are less dependent on flood characteristics. Nevertheless, LTV and LIV are highly correlated, since some intangible values (e.g. aesthetic and communal values) are sensitive to physical flood damage (e.g. lack of accessibility).

– RS (i.e. a proxy for river flow velocity) is highly correlated with LTV and LIV but not significantly correlated with MWL; therefore, both RS and MWL are crucial for accurately estimating damage.

– The robustness of these correlations is further enhanced, as testing different scales, whether varying linearly or non-linearly, yields the same results.

However, the method also presents some limitations:

– The baseline pre-disaster intangible value is obtained by combining four different typologies of value (aesthetic, historical, evidential, communal), making some assumptions to identify the criteria for assigning the level of value to each intangible aspect. Additional or alternative aspects, not currently accounted for, could influence the assignment of intangible values.

– The limited number of surveyed assets does not allow for statistically robust relationships with contributing factors. Indeed, other potential contributing factors could affect the observed damage (e.g. construction material).

The existing exposure and vulnerability models, such as those by Arrighi et al. (2023), provide reasonable initial predictions of potential damage to cultural heritage (CH). However, it should be emphasized that the available exposure data are incomplete and inadequate for identifying all the flood-exposed assets and their vulnerability, leading to inaccurate ex ante damage assessments to CH:

– In the Burano, Cesano, and Misa basins, the official flood hazard map lacks the necessary detail to distinguish which assets may suffer low or high flood damage, as it does not provide information on flood magnitude, such as water depth and velocity.

– The MIC database includes immovable and movable assets encompassing those currently under protection, as well as those under verification. Therefore, an on-site direct check, conducted in collaboration with local authorities, is always necessary to determine whether an asset qualifies as cultural heritage. Furthermore, the database does not offer any information to delineate the value of assets, and in some cases, they are not accurately geolocalized.

This paper underscores the importance of post-flood data collection and analysis. The proposed method serves as a starting point for such data collection. Nevertheless, future research should include diverse cultural and geographic contexts to improve accuracy, as the contributing factors can differently influence the observed damage. An open-source, comprehensive CH database documenting flood-related damage, asset features (e.g. construction type, and construction material), and factors describing the event magnitude (e.g. maximum water level) is needed. Additionally, quantifying tangible damage in monetary terms should allow us to obtain a more robust evaluation of the damage to CH assets. Nonetheless, it requires collaboration with government institutions to share monetary data (e.g. restoration costs). These steps would enhance flood risk management for CH conservation and help develop robust damage prediction models.

Author contributions. CA conceptualized the research idea; CA and CDL equally contributed to the planning of the on-site data collection and performed the measurements; CA, CDL, and MA developed the methodology; MA, CDL, and CA analysed the data; MA performed GIS analysis; MA handled the data visualization; CA supervised the research activity; MA and CDL wrote the manuscript draft; CA reviewed and edited the manuscript.

References

Adeyemo, O.J., Maksimovic, C., Booyan-Aaronnet, S., Leitao, J., Butler, D., and Makropoulos, C.: Sensitivity analysis of surface runoff generation for Pluvial Urban Flooding, in: 11th International Conference on Urban Drainage, 31 August–5 September 2008, Edinburgh, Scotland, UK, https://api.semanticscholar.org/CorpusID:128436486 (last access: 28 November 2024), 2008.

Alexandrakis, G., Manasakis, C., and Kampanis, N. A.: Economic and societal impacts on cultural heritage sites, resulting from natural effects and climate change, Heritage, 2, 279–305, https://doi.org/10.3390/heritage2010019, 2019.

Al-Kindi, K. M. and Alabri, Z.: Investigating the role of the key conditioning factors in flood susceptibility mapping through machine learning approaches, Earth Syst. Environ., 8, 63–81, https://doi.org/10.1007/s41748-023-00369-7, 2024.

Amaddii, M., Rosatti, G., Zugliani, D., Marzini, L., and Disperati, L.: Back-analysis of the Abbadia San Salvatore (Mt. Amiata, Italy) debris flow of 27–28 July 2019: an integrated multidisciplinary approach to a challenging case study, Geosciences, 12, 385, https://doi.org/10.3390/geosciences12100385, 2022.

Amaddii, M., Rosatti, G., Zugliani, D., Marzini, L., and Disperati, L.: Modelling stony debris flows involving culverted streams: the Abbadia San Salvatore case (Mt. Amiata, Italy), Rend. Online Soc. Geol. It., 61, 108–115, https://doi.org/10.3301/ROL.2023.55, 2023.

Anderson, K.: The impact of increased flooding caused by climate change on heritage in England and North Wales, and possible preventative measures: what could/should be done?, Built Herit., 7, 7, https://doi.org/10.1186/s43238-023-00087-z, 2023.

ANSA: Regione Marche, https://www.ansa.it/marche/notizie/2023/11/07/senigalliademolito-ponte-garibaldi-simbolo-dellalluvione-2022_c834fc28-e7c4-4e8d-9573-0346a0c13560.html (last access: 27 May 2024), 2023.

Arrighi, C.: A global scale analysis of river flood risk of UNESCO world heritage sites, Front. Water, 3, 1–12, https://doi.org/10.3389/frwa.2021.764459, 2021.

Arrighi, C.: Research Data for "Tangible and intangible ex-post assessment of flood-induced damages to cultural heritage", V1, Mendeley Data [data set], https://doi.org/10.17632/ds3xrf2npz.1, 2024.

Arrighi, C., Brugioni, M., Castelli, F., Franceschini, S., and Mazzanti, B.: Flood risk assessment in art cities: the exemplary case of Florence (Italy), J. Flood Risk Manage., 11, S616–S631, https://doi.org/10.1111/jfr3.12226, 2018.

Arrighi, C., Carraresi, A., and Castelli, F.: Resilience of art cities to flood risk: a quantitative model based on depth-idleness correlation, J. Flood Risk Manage., 15, 1–15, https://doi.org/10.1111/jfr3.12794, 2022.

Arrighi, C., Tanganelli, M., Cristofaro, M. T., Cardinali, V., Marra, A., Castelli F., and De Stefano, M.: Multi-risk assessment in a historical city, Nat. Hazards, 119, 1041–1072, https://doi.org/10.1007/s11069-021-05125-6, 2023a.

Arrighi, C., Ballio, F., and Simonelli, T.: A GIS-based flood damage index for cultural heritage, Int. J. Disast. Risk Reduct., 90, 103654, https://doi.org/10.1016/j.ijdrr.2023.103654, 2023b.

AUBAC: Autorità di bacino distrettuale dell'Appennino Centrale, https://webgis.abdac.it/portal/apps/experiencebuilder/experience/?id=c59f7b386ca24729852cf2dcf8e2f936 (last access: 28 November 2024), 2024.

Balasbaneh, A. T., Abidin, A. R. Z., Ramli, M. Z., Khaleghi, S. J., and Marsono, A. K.: Vulnerability assessment of building material against river flood water: case study in Malaysia, in: Proceedings of the 2nd International Conference on Civil & Environmental Engineering, IOP Conf. Ser.: Earth Environ. Sci., 476, 012004, https://doi.org/10.1088/1755-1315/476/1/012004, 2020.

Beven, K. J. and Kirby, M. J.: A physically based variable contributing area model of basin hydrology, Hydrolog. Sci. Bull., 24, 43–69, https://doi.org/10.1080/02626667909491834, 1979.

Brokerhof, A. W., van Leijen, R., and Gersonius, B.: Protecting built heritage against flood: mapping value density on flood hazard maps, Water, 15, 2950, https://doi.org/10.3390/w15162950, 2023.

Clini, P., Muñoz-Cádiz, J., Ferretti, U., Jiménez, J. L. D., and Nieto, G. M.: Digital transition for heritage management and dissemination: Via Flaminia and Corduba-Emerita, in: Proceedings of the 44th International Conference of Representation Disciplines Teachers, 14–16 September 2023, Milano, FrancoAngeli, 2613–2622, https://doi.org/10.3280/oa-1016-c425, 2023.

COPERNICUS: Emergency Management Service – Mapping, https://emergency.copernicus.eu/mapping/list-of-components/EMSR634 (last access: 27 May 2024), 2022.

CRED and UNISDR: The Human Cost of Weather-Related Disasters 1995–2015, https://www.preventionweb.net/files/46796_cop21weatherdisastersreport2015.pdf (last access: 19 August 2024), 2015.

Cuca, B. and Barazzetti, L.: Damages from extreme flooding events to cultural heritage and landscapes: water component estimation for Centa River (Albenga, Italy), Adv. Geosci., 45, 389–395, https://doi.org/10.5194/adgeo-45-389-2018, 2018.

Dall'Osso, F., Gonella, M., Gabbianelli, G., Withycombe, G., and Dominey-Howes, D.: A revised (PTVA) model for assessing the vulnerability of buildings to tsunami damage, Nat. Hazards Earth

Syst. Sci., 9, 1557–1565, https://doi.org/10.5194/nhess-9-1557-2009, 2009.

De Donatis, M., Lepore, G., Susini, S., Silani, M., Boschi, F., and Savelli, D.: Sistemi informativi geografici e modellazione tridimensionale per la geo-archeologia a Senigallia: nuove scoperte e nuove ipotesi, Rend. Online Soc. Geol. Ital., 19, 16–19, 2012.

De Donatis, M., Nesci, O., Savelli, D., Pappafico, G. F., and Susini, S.: Geomorphological evolution of the Sena Gallica site in the morpho-evolutive quaternary context of the northern-Marche coastal sector (Italy), Geosciences, 9, 272, https://doi.org/10.3390/geosciences9060272, 2019.

Deschaux, J.: 4 – Flood-related Impacts on cultural heritage, in: Floods, edited by: Vinet, F., Elsevier, 53–72, https://doi.org/10.1016/B978-1-78548-268-7.50004-3, 2017.

Di Salvo, C., Pennica, F., Ciotoli, G., and Cavinato, G. P.: A GIS-based procedure for preliminary mapping of pluvial flood risk at metropolitan scale, Environ. Model. Softw., 107, 64–84, https://doi.org/10.1016/j.envsoft.2018.05.020, 2018.

D.lgs. 22 gennaio 2004: n. 42, https://www.normattiva.it/esporta/attoCompleto?atto.dataPubblicazioneGazzetta=2004-02-24&atto.codiceRedazionale=004G0066 (last access: 27 May 2024), 2004.

Dottori, F., Mentaschi, L., Bianchi, A., Alfieri, L., and Feyen, L.: Cost-effective adaptation strategies to rising river flood risk in Europe, Nat. Clim. Change, 13, 196–202, https://doi.org/10.1038/s41558-022-01540-0, 2023.

Drdácký, M. F.: Impact of floods on heritage structures, J. Perform. Constr. Facil., 24, 430–431, https://doi.org/10.1061/(ASCE)CF.1943-5509.0000152, 2010.

Dutta, D., Wright, W., and Rayment, P.: Synthetic impact response functions for flood vulnerability analysis and adaptation measures in coastal zones under changing climatic conditions: a case study in Gippsland coastal region, Australia, Nat. Hazards, 59, 967–986, https://doi.org/10.1007/s11069-011-9812-x, 2011.

EU: Directive 2007/60/EC of the European Parliament and of the Council of 23 October 2007 on the Assessment and Management of Flood Risks, European Environment Agency, Copenhagen, Denmark, 27–34, https://eur-lex.europa.eu/legal-content/EN/TXT/PDF/?uri=CELEX:32007L0060 (last access: 28 November 2024), 2007.

FAI: Chiesa di Santa Maria delle Tinte, https://fondoambiente.it/luoghi/chiesa-delle-tinte?ldc (last access: 28 November 2024), 2022.

Fatorić, S. and Seekamp, E.: Are cultural heritage and resources threatened by climate change? A systematic literature review, Climatic Change, 142, 227–254, https://doi.org/10.1007/s10584-017-1929-9, 2017.

Figueiredo, R., Romǎo, X., and Paupério, E.: Flood risk assessment of cultural heritage at large spatial scales: framework and application to mainland Portugal, J. Cult. Herit., 43, 163–174, https://doi.org/10.1016/j.culher.2019.11.007, 2020.

Figueiredo, R., Romao, X., and Paupério, E.: Component-based flood vulnerability modelling for cultural heritage buildings, Int. J. Disast. Risk Reduct., 61, 102323, https://doi.org/10.1016/j.ijdrr.2021.102323, 2021.

Galasso, C., Pregnolato, P., and Parisi, F.: A model taxonomy for flood fragility and vulnerability assessment of buildings, Int. J. Disast. Risk Reduct., 53, 101985, https://doi.org/10.1016/j.ijdrr.2020.101985, 2021.

Garrote, J., Díez-Herrero, A., Escudero, C., and García I.: A framework proposal for regional-scale flood-risk assessment of cultural heritage sites and application to the Castile and León Region (Central Spain), Water, 12, 329, https://doi.org/10.3390/w12020329, 2020.

Godfrey, A., Ciurean, R. L., Van Westen, C. J., Kingma, N. C., and Glade, T.: Assessing vulnerability of buildings to hydro-meteorological hazards using an expert based approach–an application in Nehoiu Valley, Romania, Int. J. Disast. Risk Reduct., 13, 229–241, https://doi.org/10.1016/j.ijdrr.2015.06.001, 2015.

Gschnitzer, T., Gems, B., Mazzorana, B., and Aufleger, M.: Towards a robust assessment of bridge clogging processes in flood risk management, Geomorphology, 279, 128–140, https://doi.org/10.1016/j.geomorph.2016.11.002, 2017.

Historic England: Conservation Principles, Policies and Guidance, https://historicengland.org.uk/images-books/publications/conservation-principles-sustainable-management-historic (last access: 19 August 2024), 2008.

Huijbregts, Z., van Schijndel, J. W. M., Schellen, H. L., and Blades, N.: Hygrothermal modelling of flooding events within historic buildings, J. Build. Phys., 38, 170–187, https://doi.org/10.1177/1744259114532613, 2014.

Iacobucci, G., Piacentini, D., and Troiani, F.: Enhancing the identification and mapping of fluvial terraces combining geomorphological field survey with land-surface quantitative analysis, Geosciences, 12, 425, https://doi.org/10.3390/geosciences12110425, 2022.

IPCC: AR6 Synthesis Report: Climate Change 2023, https://www.ipcc.ch/report/sixth-assessment-report-cycle/ (last access: 19 August 2024), 2023.

Istituto Superiore per la Conservazione ed il Restauro: MiBACT, http://vincoliinrete.beniculturali.it/VincoliInRete/vir/bene/listabeni (last access: 27 May 2024), 2024.

Jeggle, T. and Boggero, M.: Post-disaster needs assessment (PDNA): lessons from a decade of experience, European Commission, GFDRR, UNDP, and the World Bank, http://hdl.handle.net/10986/30945 (last access: 28 November 2024), 2018.

Kefi, M., Mishra, B. K., Masago, Y., and Fukushi, K.: Analysis of flood damage and influencing factors in urban catchments: case studies in Manila, Philippines, and Jakarta, Indonesia, Nat. Hazards, 104, 2461–2487, https://doi.org/10.1007/s11069-020-04281-5, 2020.

Kreibich, H. and Thieken, A. H.: Assessment of damage caused by high groundwater inundation, Water Resour. Res., 44, W09409, https://doi.org/10.1029/2007WR006621, 2008.

Marín-García, D., Rubio-Gómez-Torga, J., Duarte-Pinheiro, M., and Moyano, J.: Simplified automatic prediction of the level of damage to similar buildings affected by river flood in a specific area, Sustain. Cities Soc., 88, 104251, https://doi.org/10.1016/j.scs.2022.104251, 2023.

Mark, O., Weesakul, S., Apirumanekul, C., Boonya Aroonet, S., and Djordjevic, S.: Potential and limitations of 1D modelling of urban flooding, J. Hydrol., 299, 284–299, https://doi.org/10.1016/j.jhydrol.2004.08.014, 2004.

Martín-Vide, J. P., Bateman, A., Berenguer, M., Ferrer-Boix, C., Amengual, A., Campillo, M., Corral, C., Llasat, M. C., Llasat-Botija, M., Gómez-Dueñas, S., Marín-Esteve, B., Núñez-González, F., Prats-Puntí, A., Ruiz-Carulla, R., and Sosa-Pérez,

R.: Large wood debris that clogged bridges followed by a sudden release, the 2019 flash flood in Catalonia, J. Hydrol.: Reg. Stud., 47, 101348, https://doi.org/10.1016/j.ejrh.2023.101348, 2023.

Marzeion, B. and Levermann, A.: Loss of cultural world heritage and currently inhabited places to sea-level rise, Environ. Res. Lett., 9, 034001, https://doi.org/10.1088/1748-9326/9/3/034001, 2014.

MASE: Geoportale Nazionale, https://gn.mase.gov.it/portale/distribuzione-dati-pst (last access: 27 May 2024), 2024.

Mastrorillo, L. and Petitta, M.: Effective infiltration variability in the Umbria-Marche carbonate aquifers of central Italy, J. Mediter. Earth Sci., 2, 4, https://doi.org/10.3304/JMES.2010.004, 2014.

Merz, B., Blöschl, G., Vorogushyn, S., Dottori, F., Aerts, J. C. J. H., Bates, P., Bertola, M., Kemter, M., Kreibich, H., Lall, U., and Macdonald, E.: Causes, impacts and patterns of disastrous river floods, Nat. Rev. Earth Environ. 2, 592–609, https://doi.org/10.1038/s43017-021-00195-3, 2021.

Molinari, D., Menoni, S., Aronica, G. T., Ballio, F., Berni, N., Pandolfo, C., Stelluti, M., and Minucci, G.: Ex post damage assessment: an Italian experience, Nat. Hazards Earth Syst. Sci., 14, 901–916, https://doi.org/10.5194/nhess-14-901-2014, 2014.

Momčilović Petronijević, A. and Petronijević, P.: Floods and Their Impact on Cultural Heritage – a Case Study of Southern and Eastern Serbia, Sustainability, 14, 14680, https://doi.org/10.3390/su142214680, 2022.

Moore, I. D., Grayson, R. B., and Ladson, A. R.: Digital terrain modeling: a review of hydrological, geomorphological, and biological applications, Hydrol. Process., 5, 3–30, https://doi.org/10.1002/hyp.3360050103, 1991.

Pulvirenti, L., Squicciarino, G., Fiori, E., Candela, L., and Puca, S.: Analysis and processing of the COSMO-SkyMed second generation images of the 2022 Marche (Central Italy) flood, Water, 15, 1353, https://doi.org/10.3390/w15071353, 2023.

Ravan, M., Revez, M. J., Pinto, I. V., Brum, P., and Birkmann, J.: A vulnerability assessment framework for cultural heritage sites: the case of the Roman ruins of Tróia, Int. J. Disast. Risk Sci., 14, 26–40, https://doi.org/10.1007/s13753-023-00463-4, 2023.

REGIONE MARCHE: Annali Idrologici, https://www.regione.marche.it/portals/0/Protezione_Civile/ManualieStudi/annale-parte-I-2021.pdf (last access: 27 May 2024), 2021.

REGIONE MARCHE: Rapporto Di Evento preliminare, https://www.regione.marche.it/portals/0/Protezione_Civile/ManualieStudi/Rapporto_Evento_preliminare_20220915.pdf (last access: 27 May 2024), 2022.

REGIONE MARCHE: Ambiente, https://www.regione.marche.it/Regione-Utile/Paesaggio-Territorio-Urbanistica/Cartografia (last access: 27 May 2024), 2023.

Reimann, L., Vafeidis, A. T., Brown, S., Hinkel, J., and Tol, R. S. J.: Mediterranean UNESCO world heritage at risk from coastal flooding and erosion due to sea-level rise, Nat. Commun., 9, 4161, https://doi.org/10.1038/s41467-018-06645-9, 2018.

Riley, S. J., DeGloria, S. D., and Elliot, R.: A terrain ruggedness index that quantifies topographic heterogeneity, Int. J. Sci., 5, 23–27, 1999.

Romão, X. and Paupério, E.: An indicator for post-disaster economic loss valuation of impacts on cultural heritage, Int. J. Archi. Herit., 15, 678–697, https://doi.org/10.1080/15583058.2019.1643948, 2021.

Romão, X., Paupério, E., Monserrat, O., Rousakis, T., and Montero, P.: Assets at risk and potential impacts: 3.6 – cultural heritage, in: Science for Disaster Risk Management 2020: Acting Today, Protecting Tomorrow, edited by: Casajus Valles, A., Marin Ferrer, M., Poljanšek, K., and Clark, I., Publications Office of the European Union, Luxembourg, 503–525, https://doi.org/10.2760/571085, 2020.

Sabbioni, C., Brimblecombe, P., Bonazza, A., Grossi, C. M., Harris, I., and Messina, P.: Mapping climate change and cultural heritage, in: Proceedings of the 7th EC Conference on Safeguarded Cultural Heritage – Understanding and Viability for the Enlarged Europe, edited by: Drdacky, M., Institute of Theoretical and Applied Mechanics of the Academy of Sciences of the Czech Republic, Prague, Czech Republic, 119–124, 2007.

Salazar, L. G. F., Romão, X., and Figueiredo, R.: A hybrid approach for the assessment of flood vulnerability of historic constructions and their contents, in: Proceedings of the Structural Analysis of Historical Constructions, SAHC 2023, RILEM Bookseries, vol. 46, edited by: Endo, Y. and Hanazato, T., Springer, Cham., https://doi.org/10.1007/978-3-031-39450-8_91, 2024.

Schlumberger, J., Ferrarin, C., Jonkman, S. N., Diaz Loaiza, M. A., Antonini, A., and Fatorić, S.: Developing a framework for the assessment of current and future flood risk in Venice, Italy, Nat. Hazards Earth Syst. Sci., 22, 2381–2400, hthttps://doi.org/10.5194/nhess-22-2381-2022, 2022.

Sesana, E., Gagnon, A. S., Ciantelli, C., Cassar, J. A., and Hughes, J. J.: Climate change impacts on cultural heritage: A literature review, WIREs Clim. Change, 12, e710, https://doi.org/10.1002/wcc.710, 2021.

Shepard, D.: A two-dimensional interpolation function for irregularly-spaced data, in: Proceedings of the 23th ACM National Conference, 27–29 August 1968, New York, NY, USA, 517–524, https://doi.org/10.1145/800186.810616, 1968.

SIRMIP ON-LINE: Sistema Informativo Regionale Meteo-Idro-Pluviometrico Regione Marche – Servizio Protezione Civile, http://app.protezionecivile.marche.it/sol/indexjs.sol?lang=it (last access: 27 May 2024), 2024.

Smith, D. I.: Flood damage estimation – a review of urban stage-damage curves and loss functions, Water SA, 20, 231–238, 1994.

Stephenson, V. and D'Ayala, D.: A new approach to flood vulnerability assessment for historic buildings in England, Nat. Hazards Earth Syst. Sci., 14, 1035–1048, https://doi.org/10.5194/nhess-14-1035-2014, 2014.

Storm Chasers Marche: L'arrivo della piena nel fiume Misa (Senigallia), https://www.youtube.com/watch?v=wNFpouu4aSg (last access: 27 May 2023), 2022.

Sulphur: Marche Mining Geopark, https://www.museosulphur.it/en/marche-mining-geopark/ (last access: 27 May 2024), 2024.

Tarquini, S., Isola, I., Favalli, M., Mazzarini, F., Bisson, M., Pareschi, M. T., and Boschi, E.: TINITALY/01: a new triangular irregular network of Italy, Ann. Geophys., 50, 407–425, https://doi.org/10.4401/ag-4424, 2007.

Tarquini, S., Isola, I., Favalli, M., Battistini, A., and Dotta, G.: TINITALY, a digital elevation model of Italy with a 10 meters cell size (Version 1.1), INGV – Istituto Nazionale di Geofisica e Vulcanologia, https://doi.org/10.13127/tinitaly/1.1, 2023.

TGCOM24: Marche, a Cantiano il ponte romano resiste al disastro, https://www.tgcom24.mediaset.it/2022/video/

alluvione-marche-a-cantiano-il-ponte-romano-resiste-al-disastro_55048806-02k.shtml (last access: 27 May 2024), 2022.

Trizio, F., Torrijo, F. J., Mileto, C., and Vegas, F.: Flood risk in a heritage city: Alzira as a case study, Water, 13, 1138, https://doi.org/10.3390/w13091138, 2021.

Vafadari, A., Philip, G., and Jennings, R. P.: Damage assessment and monitoring of cultural heritage places in a disaster and post-disaster event – a case study of Syria, Int. Arch. Photogramm. Remote Sens. Spatial Inf. Sci., XLII-2/W5, 695–701, https://doi.org/10.5194/isprs-archives-XLII-2-W5-695-2017, 2017.

Vecvagars, K.: Valuing damage and losses in cultural assets after a disaster: concept paper and research options, Naciones Unidas CEPAL – Comisión Económica para América Latina y el Caribe, 59 pp., ISBN 9211216117, 2006.

Wang, J.-J.: Flood risk maps to cultural heritage: Measures and process, J. Cult. Herit., 16, 210–220, https://doi.org/10.1016/j.culher.2014.03.002, 2015.

Willis, K. G.: The use of stated preference methods to value cultural heritage, in: Handbook of the Economics of Art and Culture, edited by: Ginsburgh, V. A. and Throsby, D., Elsevier, 145–181, https://doi.org/10.1016/B978-0-444-53776-8.00007-6, 2014.

World Events News: Terribile alluvione colpisce Marche Cantiano! Danni ad auto e abitazioni – Cantiano oggi Alluvione, https://www.youtube.com/watch?v=HjOYO-GS0dM (last access: 27 May 2024), 2022.

Zhang, S.-N., Ruan, W.-Q., Li, Y.-Q., and Xiao, H.: Cultural distortion risks at heritage sites: scale development and validation, Tourism Manage., 102, 104860, https://doi.org/10.1016/j.tourman.2023.104860, 2024.

Zugliani, D., Ataieyan, A., Rocco, R., Betemps, N., Ropele, P., and Rosatti, G.: Bridge obstruction caused by debris flow: a practical procedure for its management in debris-flow simulations, in: Proceedings of the 8th International Conference on Debris Flow Hazard Mitigation (DFHM8), 26–29 June 2023, Turin, Italy, https://doi.org/10.1051/e3sconf/202341505031, 2023.